University of Alberta
Department of Civil Engineering

Structural Engineering Report No. 72

Fatigue Behavior of Steel Beams with Welded Details

by
G.R. Bardell
and
G.L. Kulak

September, 1978

FATIGUE BEHAVIOR OF STEEL BEAMS WITH WELDED DETAILS

by

G.R. Bardell

G.L. Kulak

DEPARTMENT OF CIVIL ENGINEERING
THE UNIVERSITY OF ALBERTA
EDMONTON, ALBERTA

SEPTEMBER, 1978

ABSTRACT

This investigation was established in order to examine the fatigue behavior of two commonly-used welded steel details. The present design specifications of the American Association of State Highway and Transportation Officials, Standard 1977, and the Canadian Standards Association, Standard S6-1976, classify these details based on past experience and judgement rather than by explicit testing. As a consequence, the performance of these details under fatigue loading is uncertain.

The results of tests on 18 beams with groove-welded flange splices and seven beams with lateral bracing attachment details are presented. This study indicates that the present classification of groove-welded splices with the weld reinforcement removed and also the classification of fillet-welded attachments are both adequate in the current specifications. The study indicates, however, that the present classification of groove-welded splices with the weld reinforcement left as-welded may be overly conservative.

In addition to the above, the tests on beams with lateral bracing details were conducted in such a way as to ascertain the effects of attaching bracing members to these details. Based on the scope of the program carried out it was concluded that the attachment of bracing to the lateral gusset detail has no influence on the fatigue life of the beam.

ACKNOWLEDGEMENTS

This study was carried out in the Department of Civil Engineering at the University of Alberta. It was conducted with the financial assistance of the Canadian Steel Industries Construction Council.

The authors wish to express their thanks to the technical staff of the Department of Civil Engineering for their assistance during the testing program.

The senior author would also like to thank the Roads and Transportation Association of Canada for the financial assistance which he received from them during the time this study was being completed.

TABLE OF CONTENTS

CHAPTER I

INTRODUCTION

1.1 General

Fatigue may be considered as a progressive type of failure, originating from micro-cracks or dislocations in the structure of the material and growing into visible cracks by the repeated application of stresses. These stresses are less than the general yield stress of the uncracked portion of the section. Once the cracks have increased sufficiently in size, structural failure may then result as the stresses on the uncracked portion exceed some failure value.

Fatigue cracking can be a serious problem in modern highway or railway bridge structures which are often subjected to several millions of cycles of heavy loads over the life of the structure. Although fatigue cracking is not a common problem in these structures, if it does occur it can result in sudden and catastrophic failure, and consequently must be considered as an integral segment of the design process.

Knowledge of the failure strength of steel beams has increased considerably in recent years. Mainly as a result of work done under the National Cooperative Highway Research Program (NCHRP) in the United States, the current approach to design of steel beams for fatigue represents a substantial

improvement over that used previously. Prior to the "Interim Standard Specification for Highway Bridges, AASHTO 1974" (1), the design of steel bridges for fatigue was based essentially on the concept of stress ratio for a limited number of fatigue categories. Fisher, et al. (2,3), showed that the stress range rather than the stress ratio was the dominant factor determining fatigue strength. These investigators also identified and classified major design details into six categories based on the severity of stress concentration. Furthermore, they outlined the factors which have little or no effect on fatigue strength but which were previous considerations in design.

It is now generally accepted that the major factors governing fatigue strength of structural steel members are the applied stress range, the number of cycles and the type of detail (4,5).

1.2 Statement of Problem

The present bridge design codes of the American Association of State Highway and Transportation Officials (AASHTO) (4) and the Canadian Standards Association (CSA) (5), as well as the Canadian design code for steel buildings (CSA S16.1) (6), are all based on the NCHRP tests (2,3). Basically, these specifications group all details into one of six categories according to fatigue strength. The 95% confidence limit for 95% survival of a typical detail in each of the categories is used as the design criterion. An allowable stress range is given for a certain number of loading cycles.

The rapid development of this present method of fatigue design has meant that many types of details commonly used in Canadian practice have only been included implicitly in the codes, or have been categorized by engineering judgement without adequate testing. Consequently, some of these details may be overly conservative or conversely may not have a sufficient factor of safety against failure.

1.3 Objectives

The objectives of this investigation are:

1. To examine the fatigue strength of two commonly used details by means of a suitable testing program. As will be described in Chapter III, the details to be tested are groove-welded splices and fillet-welded attachments of the type commonly used for connection of horizontal bracing to main girder members.

2. To analyse the test results using a fracture mechanics approach.

3. To compare test results with those previously obtained for similar details and with the predicted fatigue strength using the various design specifications.

4. To suggest revisions to the present design specifications, if appropriate.

5. To make recommendations for future testing.

CHAPTER II

LITERATURE SURVEY

2.1 Early Investigations

Since the middle of the nineteenth century, failure by fatigue has been recognized as a potential problem in steel elements. Most of the early recognized fatigue failures occurred in machine parts or axles which were subjected to frequent vibrations and/or cyclic loads. Relatively few failures occurred in civil engineering structures such as bridges and buildings. As a logical consequence of this, most of the early testing and fatigue investigations involved shafts or other rotating machine parts.

With the development and acceptance of welded steel structures, longer, more slender bridges became common. As welded joints and connections in these structures generally result in more critical notch-producing details than comparable details in riveted truss systems, the appearance of fatigue cracks became more prevalent. In addition, the bridges were probably being subjected to a larger number of load cycles at higher loads as various highway authorities permitted larger vehicles, and this also contributed to the fatigue problem. Consequently, the increasing incidence of fatigue cracking has necessitated more fatigue tests on structural type details in the last few decades.

Generally, these fatigue tests have been very limited in scope. An important limitation of many of these tests is that too many variables were included in one test. Thus, isolating those parameters which were affecting the fatigue strength became difficult.

2.2 Development of Present Code Requirements

In the late 1960's and early 1970's an extensive series of tests on the fatigue strength of steel beams was conducted at Lehigh and Drexel Universities in the United States under the National Cooperative Highway Research Program (2,3).

The major objective of this investigation was to develop quantitative design relationships for the fatigue strength of steel beams. Over 500 beams with one or more details were tested in two separate studies. The principal design variables were type of steel, stress condition, and type of detail. The details tested included plain-rolled beams, plain-welded beams, and beams with cover-plates, stiffeners, splices, and flange attachments. The test program was statistically designed such that the significance of each design variable could be ascertained.

It was found that the major factors influencing the fatigue strength were the applied stress range, the number of cycles, and the type of detail. The initial flaw size was also shown to be a major contributing factor. The type of steel had little, if any, effect on the fatigue strength. (The structural

steels tested had yield strengths ranging from 36 ksi to 100 ksi.) Other factors showing no significant effect on fatigue life included rest periods or interruptions of the test, loading frequency, laboratory temperature and humidity.

When the test results were plotted on a log-log scale of stress range versus number of cycles, the regression lines for the various details were essentially parallel with a negative slope of approximately 3.0. The upper bound to the family of lines, that is, the highest fatigue strength, was found to pertain to the plain-rolled beam with no details attached, and the lower bound (the lowest fatigue strength) represented the cover-plated beam. Between these two limiting details were, in decreasing order of fatigue strength, beams with splices, with stiffeners, and those with flange attachments.

The 1974 Interim Standard Specification for Highway Bridges (1), published by AASHTO was essentially based on the above series of tests. In this specification, the number of stress cycles to be used in design is a function of the bridge location and the type of member. It is then left to the designer to choose the type of detail and/or to limit the stress range in order to satisfy the code requirements.

The types of details are grouped into six categories (A to F) which have similar fatigue strengths. Many of these details were tested in the Lehigh and Drexel program but some were merely categorized qualitatively using engineering

judgement (2,3). Restricting the types of details to only six categories was essentially a means of simplifying the design process.

The selection of the allowable stress range for the various categories was based on the lower limits of dispersion in the test results. This lower limit was the 95% confidence limit for 95% survival. For each of the six categories, a permissible stress range was selected from this lower line for the commonly used load cycle categories of 100,000, 500,000, 2,000,000, and over 2,000,000 cycles. These values were then presented in tabular form.

In summary, design for fatigue according to the 1974 AASHTO Specifications, consists of three basic steps. First, the number of stress cycles is selected depending on the type of roadway and the type of structural member to be designed. Secondly, the fatigue category for the particular type of detail is determined. Thirdly, the actual design stress range is checked against the permissible stress range given for that particular stress category and number of stress cycles. If the design stress range exceeds that allowed in the specifications, then the designer has two options. The type of detail can be changed in order to fall into a less critical fatigue category or the member size can be increased in order to reduce the stress range.

Supplement Number 1-1976 to CSA Standard S6-1974, Design of Highway Bridges (5) and CSA Standard S16.1-1974 Steel

Structures for Buildings - Limit States Design (6), provide specifications for fatigue design that are similar in most respects to those just described.

2.3 Previous Testing of Sections with Groove-Welded Splices

A significant number of tests have been carried out on sections with groove-welded butt splices. Most of the early tests, however, were done using tension tests on spliced plates. Both Gurney (7) and Munse (8) found that removal of the weld reinforcement resulted in increased fatigue strength. Tension tests, however are not necessarily representative of the fatigue strength of beams in bending. Differences include such factors as the stress gradient effect in beams, the redistribution of stresses to different locations in a beam after cracking occurs, and the greater probability that flaws will exist in a beam section. In addition, many of the early tests were done on tension specimens with machined surfaces. This would tend to reduce the number and size of initial flaws and consequently increase the fatigue strength.

In the early 1960's, tests were conducted at the University of Illinois on approximately 100 beams with groove-welded butt splices (9). The details examined included placing in-line or staggering of web and flange welds, and the effect of having cope holes around the weld. The majority of these beams had the reinforcement left in place so its effect on the fatigue strength was not specifically evaluated.

A number of other tests have been carried out on beams with thickness or width transitions at the groove-welded splice. Fisher et al. (2), observed that a 2 ft radius transition in width or a 2-1/2:1 taper with the reinforcement removed, resulted in essentially the same fatigue strength as a plain-welded beam. Yamada and Albrecht (10), observed that a 4:1 taper in thickness transition for groove-welded splices again provided the fatigue strength of a plain-welded beam.

Recent studies of beams containing groove welds have tended to concentrate on thickness or width transitions or on the effect of copes in beam splices. Several variables have often been included in one test so that isolating the effect of any one variable becomes difficult. An example of this is a thickness transition in combination with a groove-welded splice. No studies to date have isolated the effects on fatigue strength of leaving the groove weld reinforcement on a beam section. It is the purpose of this study to isolate this effect, thus comparing beam splices containing as-welded groove welds with beam splices in which the groove weld has been ground flush, and also comparing both of these details with the fatigue strength of a similar size plain-welded beam.

2.4 Previous Testing of Sections with Fillet-Welded Attachments

Prior to the Lehigh-Drexel test series in the early 1970's (3), relatively few tests had been carried out on beams

with fillet-welded attachments. Of the tests that were done, many were conducted as tension tests on flat-plate specimens (25,26,27). These plates usually had short gussets attached to the surface or the edge of the plate, with the majority oriented parallel to the direction of stress. The main observation drawn from these tests was that a decrease in the size of the attachment improved the fatigue strength.

The Lehigh-Drexel tests involved a series of approximately 50 beams with attachments fillet-welded to the tension flange (3). These attachments varied in length from 1/4 in. to 8 in. measured in the direction parallel to the bending stress. It was again observed that the fatigue strength decreased as the attachment length increased. Even the 1/4 in. attachment reduced the fatigue strength considerably from that of a plain-welded beam. This length effect was attributed to the force development in the attachment plate. In all of these tests the failure resulted as a consequence of a crack originating at the toe of the attachment fillet weld. Based on this test series, the AASHTO 1974 Interim Specifications classified fillet-welded attachments as either fatigue category C, D, or E, depending on the length of attachment (1).

All of the fatigue classifications mentioned above were established as a result of tests carried out on beams with attachments to the flange. Attachments to the web are included in these categories, although no studies on this type of

detail have been reported to date. A major purpose of this study is to examine the fatigue strength of a web attachment as frequently used on highway and railway bridges.

Another important consideration for fatigue design is the effect of secondary stresses due to differential girder deflections. The failure of the Lafayette Street Bridge (11) has prompted concern for examination of connection details and the effects of secondary stresses (12). This study will attempt to examine one such detail and determine the effect upon fatigue life of differential girder displacement. This differential girder displacement will introduce both axial forces in the lateral bracing system, and hence in the welded attachment on the girder, and also produce rotation of the attachment.

CHAPTER III

EXPERIMENTAL PROGRAM

3.1 Scope

As has been described, the purpose of this project was to examine the influence of two different types of details upon the fatigue strength of steel beams. These will be referred to throughout the remainder of this report as Phase 1 and Phase 2.

Phase 1 was an examination of the effect of groove-welded flange plates upon the fatigue strength of beams. The purpose of the study was to determine the effects of grinding flush the weld reinforcement on a groove-welded splice as compared to leaving the splice as-welded and also to compare these details with the fatigue strength of a plain-welded beam. The test series consisted of 18 specimens, all of which were welded, built-up beams. Nine of the beams had an as-welded groove weld across the tension flange while the remaining nine had a similar detail but one in which the groove-weld reinforcement was ground flush with the profile of the flange. Six specimens were tested at each of three stress ranges.

Phase 2 was an investigation of the fatigue strength of beams with horizontal bracing attachment details. This study consisted of an evaluation of the effects of the detail itself, and also considered the detail in conjunction with lateral

bracing attached. The latter was an attempt to simulate the rotation of bracing attachments on a bridge due to differential girder deflections. The test series consisted of seven specimens, all rolled steel beams. Each beam had two attachment details, one on each side of the beam web. The seven beams were tested at various stress ranges.

3.2 Phase 1 (Beams with Groove-Welded Splices)

3.2.1 Specimen Description

All 18 test beams were fabricated by the Dominion Bridge Company Limited at their Edmonton plant. The fabricator was instructed as to the type of material and method of fabrication to be used.

All steel was to meet the specifications of CSA G40.21 44W. The specimens consisted of built-up beams 10 ft 6 in. long and made up of a 1 ft 1-1/16 in. by 1/4 in. web plate with 6-3/4 in. by 3/8 in. flange plates.

All welds (except tack welds) were made by the automatic submerged arc process using AWS E70XX electrodes. The flange plates were welded to the web plate using continuous 3/16 in. fillet welds. All 18 beams were fabricated with a full-penetration, groove-welded butt splice in the bottom flange at midspan. This groove weld was made prior to assembly of the web and flange plates and was made on the source plate prior to cutting the flanges to the required width. The source plate was then trimmed

a minimum of one inch on each side after welding in order to eliminate the effects of starting and stopping the weld. The groove welds were all made using a steel backing strip; this strip was then removed and the weld back-gouged and back-welded to ensure full penetration of the weld. The groove-welds were inspected using an X-ray method.

The groove weld face reinforcement was ground flush with the bottom flange profile in nine of the specimens. This grinding was done in the longitudinal direction of the flange plate (that is, in the direction in which the bending stress was to be applied). In the remaining nine specimens the plates were assembled with the groove-weld left as-welded. Figures 3.1 and 3.2 show the groove-welds, as-welded and ground flush, respectively.

3.2.2 Test Set-Up

All specimens were tested on a 10 ft span with two-point loading at the centre of the span. The distance between the loading points was 2 ft and the groove weld was contained within this region of constant moment.

The specimens were all simply-supported at the reaction points. Steel rockers were used both at the reactions and at the two loading points.

Loading was applied by means of an Amsler system. This system uses a variable-stroke hydraulic pump (a pulsator) to

load the jacks. The pump has two fixed operating speeds of 250 and 500 cycles-per-minute. The 500 cycle-per-minute speed was used for the entire test series. The maximum dynamic capacity of the jack is 110 kips.

As shown in Fig. 3.3, the load was applied to the beam through a spreader beam by a single jack. At the lower stress ranges it was possible to conduct tests in which two beams were tested simultaneously by two jacks applying identical loads.

The loads necessary to produce the required stresses were determined by calibrating the minimum and maximum load dial gauges on the Amsler unit. A strain gauge was mounted on the bottom flange of each test beam at midspan and the loads were then applied statically to the beam. When the required strain was reached, as indicated by the strain gauges, then that value was marked on an oscilloscope connected to the gauge. Two lines were marked on the oscilloscope corresponding to the minimum and maximum stresses. The pulsator was then started and loads were applied dynamically until the required stresses were reached as previously marked on the oscilloscope. These loads were then recorded on the dial gauges of the Amsler unit and subsequently used for future loadings with the same stress range.

3.2.3 Testing Procedure

The principal design variables for this study were type of detail (ground flush versus as-welded groove welds) and stress range.

Six specimens (three of the as-welded and three with the weld ground flush) were tested at each of three stress ranges. Selection of the upper and lower stress ranges included consideration of jack capacity and testing time as well as the requirement that as much as possible of the stress range versus number of cycles relationship be developed. Stress ranges of 17 ksi, 25 ksi and 32 ksi were used. The minimum stress in all cases was 8 ksi, therefore the maximum stresses were 25 ksi, 33 ksi and 40 ksi, respectively.

The criterion used to define failure in this test series was an increase in midspan deflection. This was the same failure criterion as was used in the Lehigh and Drexel programs (2,3). An increase in midspan deflection of 0.020 inches was found to result from a crack size considered to be failure of the section. The cracked area was approximately equal to 50% to 80% of the flange area at that point.

The majority of the tests were run continuously, 24 hours a day, without interruption until failure occurred. Several tests were interrupted, however, for periods ranging from several hours to a week or more. A microswitch was set under each beam which would automatically stop the loading when the deflection failure criterion was reached.

Prior to the testing, two series of standard coupon tests were conducted to determine the material properties. Loose pieces of material were supplied from both the web and flange

plates. These pieces were taken parallel to the long direction of the source plate. Three coupon tests were performed on each of the web and flange plate materials. Each coupon was loaded until the material had just entered the range of yielding. The strain was then held constant while the coupon was allowed to relax causing a reduction in the load. Once the load had stabilized, this value was then recorded as the static yield point. The procedure was repeated two more times to obtain an average reading. The average static yield point was found to be 55.2 ksi for the web material and 42.7 ksi for the flange material.

3.3 Phase 2 (Beams with Lateral Bracing Attachments)

3.3.1 Specimen Description

All seven test beams were W16 x 36 hot-rolled wide-flange sections, 10 ft 6 in. in length. All steel was to meet the specifications of CSA G40.21 44W. Each beam had a vertical stiffener and a horizontal gusset plate welded on each side of the web. All the stiffeners and gusset plate attachments were welded to the beams at the University of Alberta Structural Engineering Laboratory by a welder certified by the Canadian Welding Bureau.

Figures 3.4 and 3.5 show the attachment detail and vertical stiffener. The vertical stiffeners were 3/8 in. thick plates, 3-1/4 in. wide and either 12-1/2 in. or 13-1/2 in. long.

These stiffeners were fillet welded to the top flange of the beam and to the beam web. A 1 in. by 1 in. cope was cut out of the top corner of each stiffener to prevent contact between the flange and web welds. Each stiffener was located 9 in. from the centre line of the beam span, on opposite sides of the web, and were placed antisymmetrically.

The horizontal gusset plates were 4-3/4 in. wide by 10 in. long steel plates, 5/16 in. thick on five of the beams and 3/8 in. thick on the remaining two beams. A slot was saw cut out of the centre portion of each gusset so it could be fitted over the vertical stiffener. The gusset plates were fillet welded to the beam web and to the stiffener. A 1 in. by 1 in. cope was cut out of the centre portion of each gusset to prevent contact between the web and stiffener welds. Six of the beams had the gusset plate attached at a distance of 2-7/16 in. from the extreme fibre to the underside of the gusset. The seventh beam had one of its gusset plates attached at a 2-7/16 in. distance, and the gusset on the opposite side of the web attached at a 3-7/16 in. distance from the extreme fibre.

All welds were done manually by the shielded-metal-arc process using AWS E70XX electrodes. The fillet welds were 1/4 in. in size. A visual inspection of all fillet welds was conducted prior to testing.

3.3.2 Test Set-Up

All specimens were tested on a 10 ft span with two-point loading at the centre of the span. The distance between the loading points was 3 ft 6 in. Both horizontal attachment details were in the constant moment region. The specimens were all simply-supported on steel rockers at load and reaction points.

Each test was conducted with angles bolted to the gusset plate on one side of the beam while the detail on the opposite side of the beam had no such attachment. The angles extended outward at 45° to the beam axis and had their far ends clamped to a pedestal at a fixed elevation. Figures 3.6 and 3.7 show these bracing angles. The angles represented an attempt to simulate the lateral bracing on a bridge member in order to determine the effects of forces in these bracing members due to differential girder deflections. Angles were only attached on one side of the beam so that the effects on the fatigue strength of the beam of bracing angles in conjunction with the gusset plate could be isolated from the effects of the gusset plate detail only.

The first beam tested, specimen L-1, had 2-1/2 in. x 2-1/2 in. x 1/4 in. angles bolted to the gusset plate and clamped to a pedestal at a diagonal distance of 25 in. from the bolts. For the remaining six beams, 2-1/2 in. x 2-1/2 in. x 3/8 in. angles were bolted to the gusset plate and clamped at a diagonal distance of 70 in. from the bolts. It was felt that the latter test set-up gave a closer approximation to the bracing

stiffness of an actual bridge member. Prior to these latter six tests, a field survey was conducted on two bridges in the Edmonton area to determine differential girder deflections under heavy truck loading and the relative stiffness of the bracing. Details of this survey are given in Appendix A.

The application and measurement of load was similar to that described for the Phase 1 tests. A loading speed of 500 cycles-per-minute was used for the entire test series.

3.3.3 Testing Procedure

The stress at the level of the gusset plate was approximately 70% of the extreme fibre stress in the beam. For the seven specimens, various stress ranges were applied and these ranged from 9 ksi to 19.5 ksi at the level of the gusset plates. A minimum extreme fibre stress of 4 ksi (2.8 ksi at the gusset plate) was used in all cases.

The principal design variables for this study were stress range and type of detail (gusset plate versus gusset plate plus lateral bracing).

Prior to the fatigue testing, static tests were conducted on most specimens. Strain gauges were mounted on both gusset plates to determine the stress distributions due to flexure of the beam and due to the forces in the bracing angles. Deflection gauges were set up beneath the beam and beneath the gusset plate. The specimen was then loaded statically and

measurements of strains and deflections were recorded for various load increments.

Upon completion of the static tests, the deflection gauges were removed and the beam was then loaded dynamically to the required stress range, as calibrated previously.

The failure criterion for this test series was again somewhat arbitrary. Failure was considered to have occurred when the observed crack in the beam web was essentially the same size on both sides of the web, that is, when the crack had grown through the web thickness. The cracks were usually 1 in. to 1-1/2 in. long at this point.

This criterion was chosen so that the test could be stopped and the cracks repaired in order that testing might continue with a view to obtaining similar cracks at other locations. When a test was stopped, the crack area was reinforced with weld material and the section modulus was increased locally in that area by clamping plates to the bottom flange. By repairing the cracks and continuing the tests, up to four independent fatigue cracks occurred in each specimen.

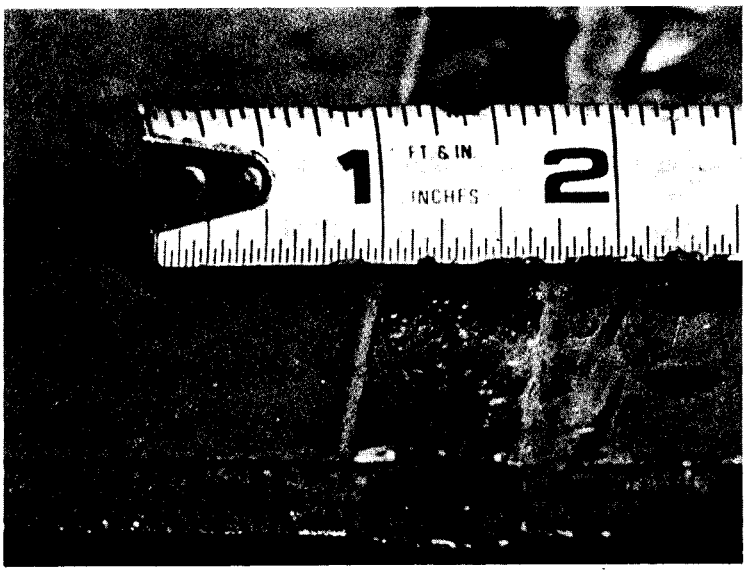

FIGURE 3.1 GROOVE WELD: AS-WELDED

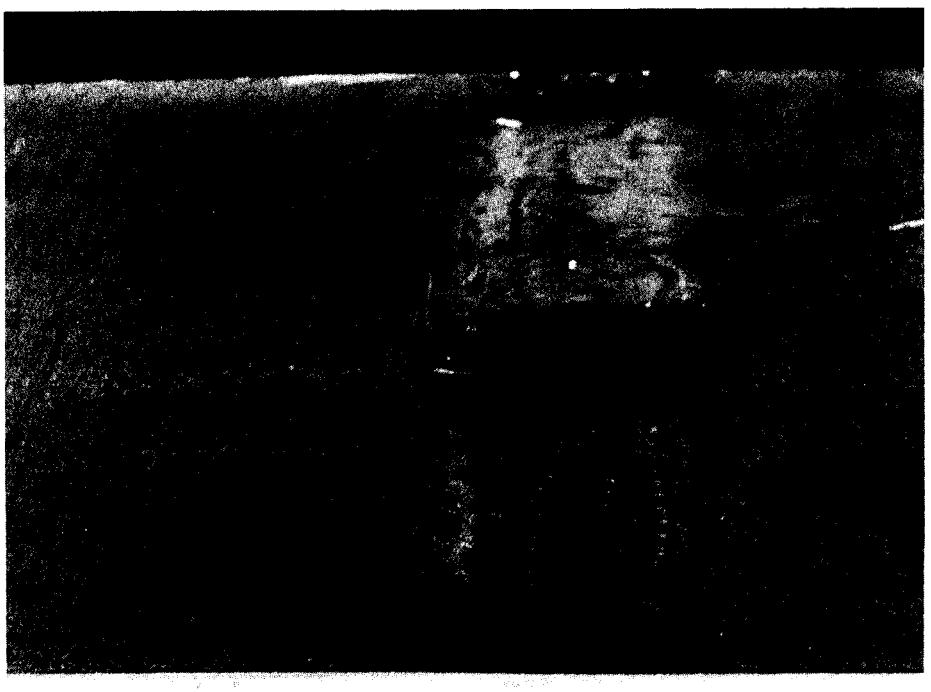

FIGURE 3.2 GROOVE WELD: GROUND FLUSH

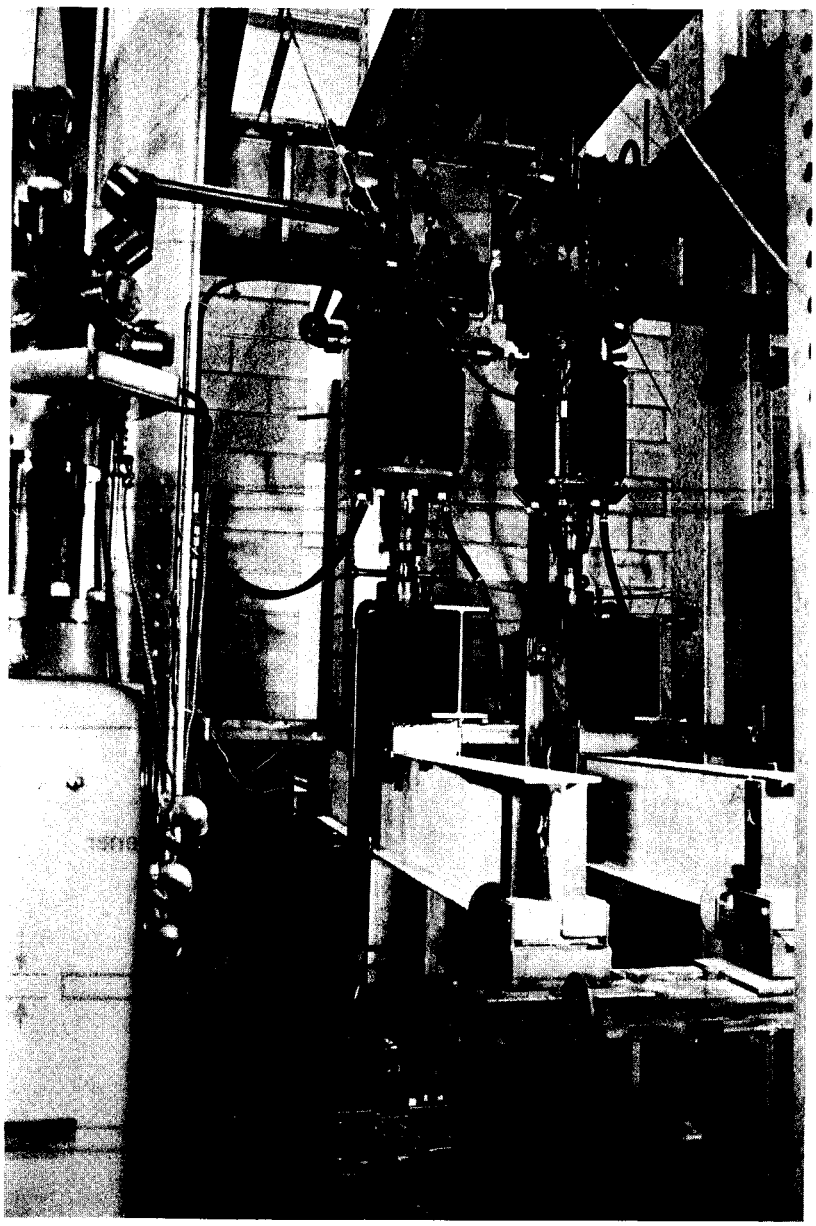

FIGURE 3.3 TEST SET-UP

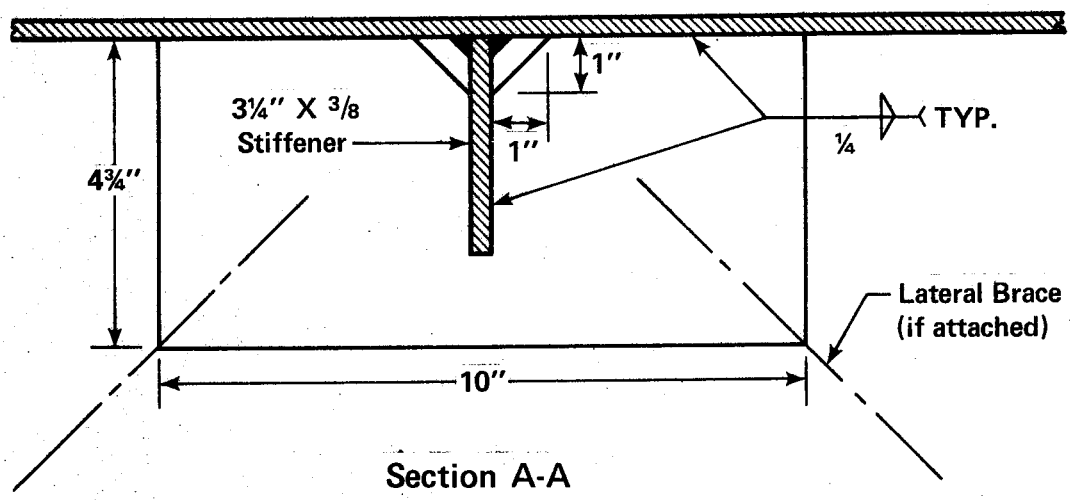

Section A-A

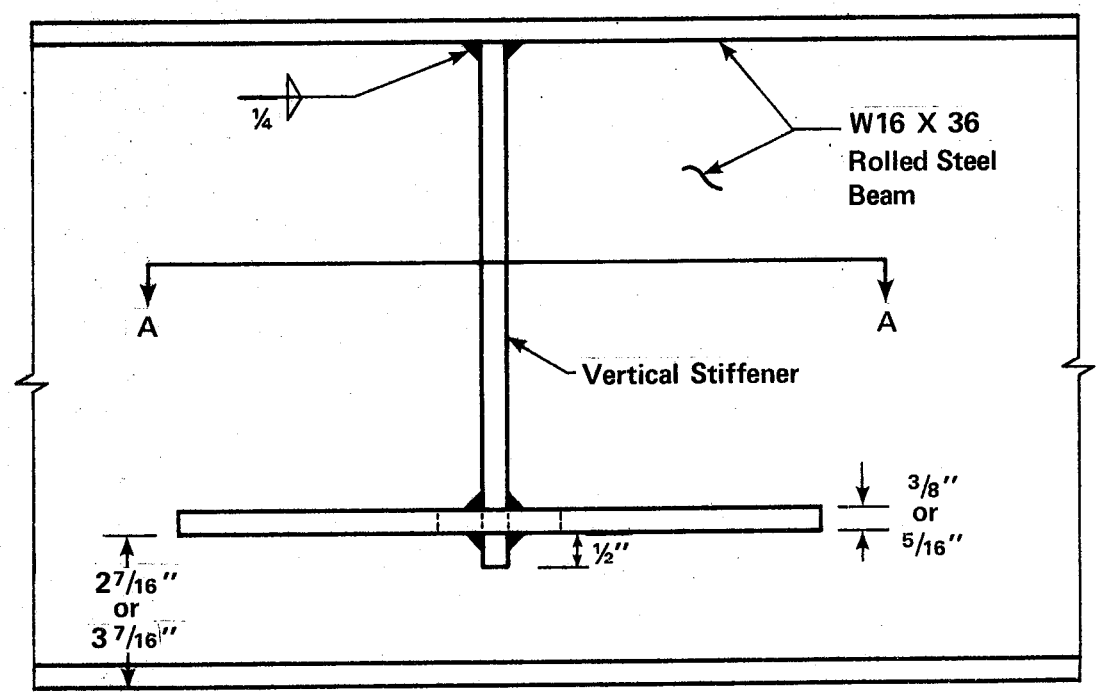

Elevation

FIGURE 3.4 LATERAL BRACING ATTACHMENT DETAILS

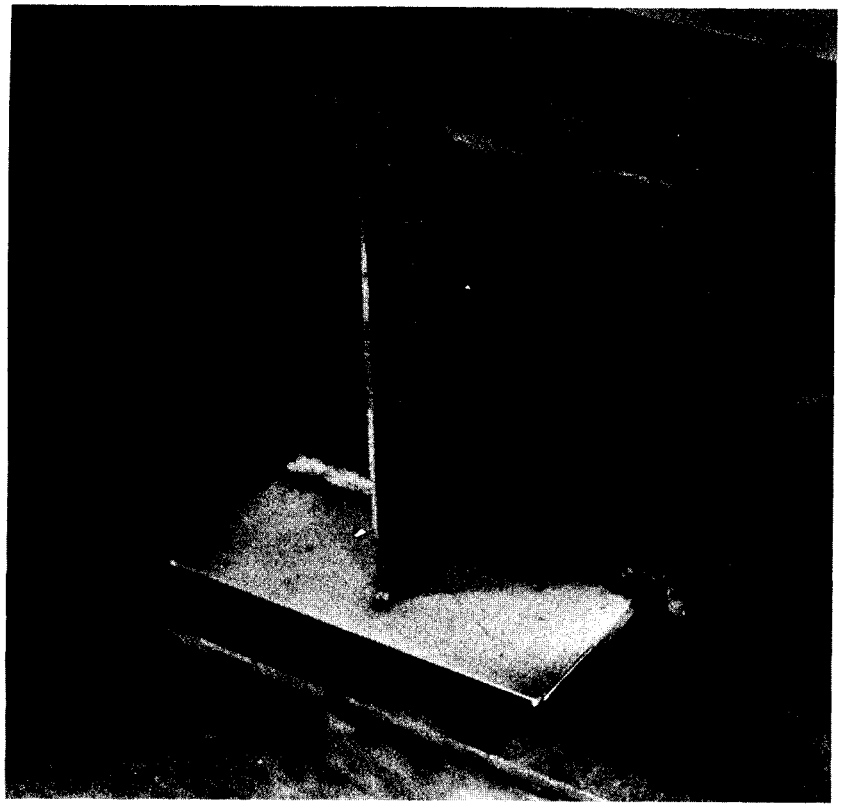

FIGURE 3.5 LATERAL BRACING ATTACHMENT

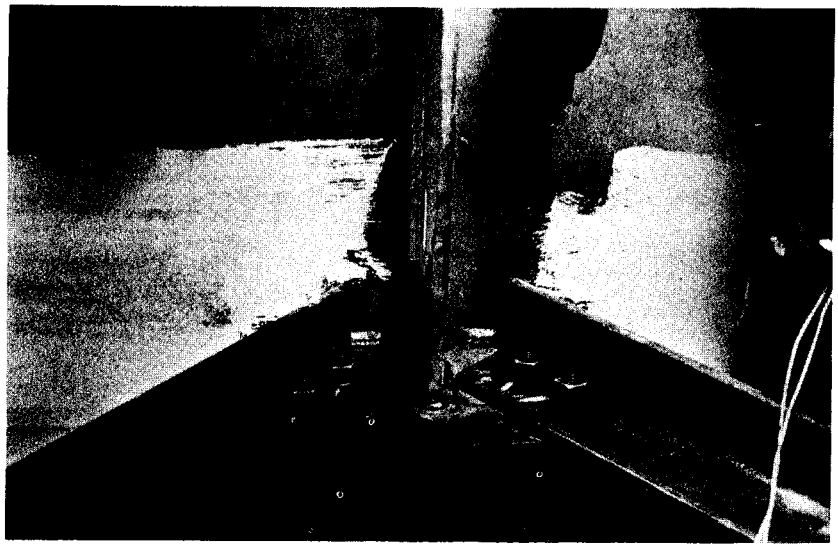

FIGURE 3.6 BRACING ANGLE DETAIL

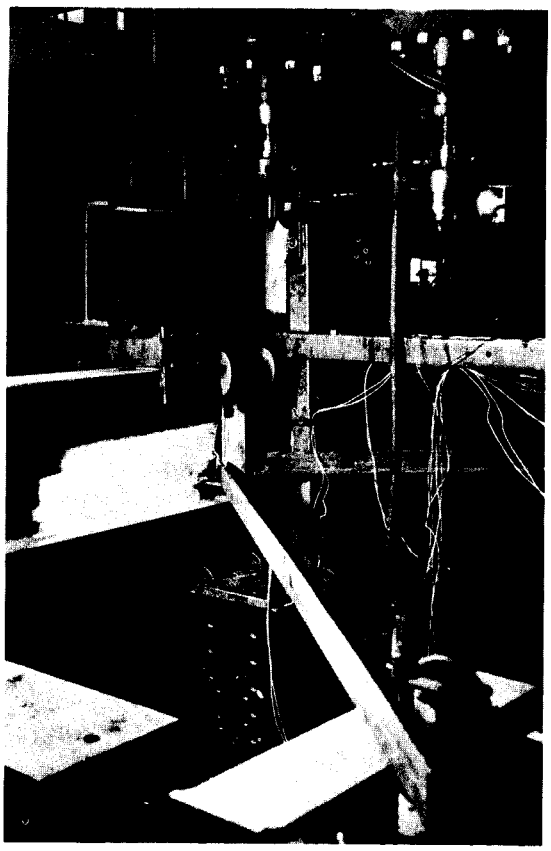

FIGURE 3.7 BRACING ANGLES

CHAPTER IV

TEST RESULTS

4.1 Phase 1 (Beams with Groove-Welded Splices)

4.1.1 Crack Initiation and Growth

None of the nine beams tested with flush-ground groove welds failed as a result of a crack initiating at the groove weld. In seven of these beams, the failure crack started in the fillet weld at the web-to-flange junction. In the other two cases, failure resulted from cracks initiating at notches in the flange tip.

The flaws in the flange-to-web fillet weld which initiated the fatigue cracks were slag inclusions and/or gas pockets or porosity. The cracks starting from these flaws grew through the fillet weld, (at which time they became visible to the observer), and then, simultaneously, vertically through the web and horizontally towards both flange tips. The web crack grew much more slowly than the flange crack with growth effectively stopping after reaching a length of one to two inches. This was due to the stress gradient from bending which resulted in lower stresses as the crack propagated away from the bottom flange. Figure 4.1 shows typical cracks of this type.

In the two beams with edge notches, the failure crack initiated at the flange tip and propagated through the flange and

towards the web. Figure 4.2 illustrates this type of failure (Fig. 4.7 shows the type of notch which initiates this form of cracking). Failure of the beam occurred prior to these cracks reaching the web. Thus, this type of crack grew in only one direction.

Prior to testing, an attempt was made to prevent the crack from forming at the notch in one of the edge-notched beams. This was done by locally reinforcing the section using steel plates clamped to the bottom flange over the notched area. This proved unsuccessful since a crack did appear and grow from the flange tip. However, this specimen did exhibit a slightly higher fatigue life than the unclamped, notched beam. Both of the notched beams had lower fatigue strengths than the unnotched beams tested at the same stress range.

Failure of these beams was considered to have occurred when the dynamic deflection increased by 0.020 inches. At this stage the crack generally extended through 50 to 80% of the tension flange.

None of the fatigue cracks in any of the nine beams of this type occurred in the vicinity of the groove-welded splice nor in the region of grinding of the weld reinforcement.

In the test beams with the groove weld left as-welded, the crack causing failure initiated at one of three locations (See Table 4.1). At high and medium stress ranges, the crack in six of the nine beams started at the flange tip, at the toe

of the groove weld reinforcement. Of the remaining beams, two which were tested at the low stress range failed from a crack initiating in the flange-to-web fillet weld. This failure was similar to that described previously for the flush ground groove-welded beams. The ninth beam failed from a crack initiating at a distinct flaw in the groove weld.

There were no noticeable flaws in the groove welds of those beams in which the cracks initiated at the flange tips. The cracks generally started at the toe of the groove weld in locations where the curvature at the toe of the reinforcement was the greatest. This was especially noticeable at those locations where the transition in thickness to the reinforcement was abrupt. These cracks propagated from the flange tip toward the web, along the toe of the reinforcement. Failure of the beam generally occurred when the fatigue crack reached the vicinity of the web, that is, with approximately 50% of the tension flange cracked. Figure 4.3 shows a failure crack of this type.

In the two beams in which cracks initiated in the flange-to-web fillet weld, the type of failure was similar to that of the beams with the groove weld ground flush. The crack grew through the fillet weld and then grew simultaneously through the web and towards both flange tips. In neither of the two beams did the crack occur in the vicinity of the groove-welded splice.

In the ninth beam, which was tested at the low stress range, there was a slight undercut at the toe of the groove weld

which initiated failure. This undercut was probably due to an interruption in the automatic welding process. The flaw was detected in the weld inspection and a repair was made. Nevertheless, the crack still initiated at this location, which was at the toe of the groove weld reinforcement, approximately half-way between the flange tip and the web. The crack grew simultaneously from this location towards the flange tip and towards the web.

In one of the beams tested at the lower stress range, several cracks also occurred in the compression flange area beneath the load point rockers. These cracks started at the centre of the compression flange over the web. They then propagated through the web until they reached a length of approximately 1-1/2 in. No further growth occurred after this time.

In all of the beams tested in this phase, it was observed that the majority of the fatigue life was spent propagating the cracks to the surface of the material. This was particularly noticeable for those cracks initiating in the flange-to-web fillet weld, where over 95% of the life was consumed before the cracks were visible at the surface of the weld.

4.1.2 Effect of Stress Range

As expected, the test data show that stress range has a major effect on the fatigue lives of these beams. In the

extensive series of tests carried out by Fisher et al., it was observed that the maximum and minimum stresses did not significantly affect the fatigue life, and that the stress range was the predominant factor (2,3). Consequently, for this series of tests, the minimum stress was maintained at a constant value and only the stress range was varied. It was observed that the fatigue life decreased as the stress range increased.

Figure 4.4 summarizes the test data for the beams with the groove welds ground flush. (Table 4.1 gives a complete summary of the test series.) A linear regression analysis was carried out on the test data using a least squares fit. The linear model used was Log $N = B_1 + B_2$ Log Sr. The solid line in Fig. 4.4 represents the mean regression line for the nine beams of this type. The dashed line represents the mean regression line for eight beams, excluding beam GF-7, which failed at a significantly lower number of cycles due to crack propagation from the notch in the flange tip. The equations for the regression lines are shown on the figure.

Figure 4.5 summarizes the test data for the beams with the groove welds left as-welded. The solid line represents the mean regression line for the nine beams of this type. The dashed line represents the mean regression line for eight beams, excluding beam AW-2, which failed at a significantly lower number of cycles due to crack initiation at the groove weld undercut.

No fatigue limit was reached for any of the beams tested. (The fatigue limit is the value of the stress range below which the specimen can apparently endure an unlimited number of cycles without failure.) This limit did not occur for either of the types of beams tested, although several beams had fatigue lives of over five million cycles.

4.1.3 Effect of Groove Weld Detail

It is apparent from the test data results (shown in Fig. 4.6) that, with a few exceptions, the beams with the groove weld reinforcement ground flush resulted in somewhat higher fatigue strengths than those with the groove weld left as-welded. The regression lines for the two types of details were almost parallel. The slope of the regression line for the as-welded beams in Fig. 4.5, using eight data points (excluding beam AW-2), had a greater slope than that of the ground flush detail. This resulted in the two lines tending to converge in the lower stress ranges, and probably would account for the similar failure modes for beams in that region of the plot.

The type of failure was generally different for the two details. In the flush-ground beams, the majority of the cracks initiated in the flange-to-web fillet weld, at locations away from the groove-welded splice. This is similar to the type of failure described by Fisher et al. for plain-welded beams with no splice (2). In the as-welded beams, the fatigue cracks generally initiated at the toe of the groove weld

reinforcement for the high and medium stress ranges, and in the flange-to-web fillet weld at locations away from the groove weld for the low stress range. The exceptions to the above types of failure were in those beams where failure initiated at a notch in the flange tip or at a flaw in the groove weld.

The scatter in data points was noticeably less for the as-welded beams than for those with the weld ground flush. This is further emphasized by the difference in correlation coefficients (R^2). The as-welded beams had an R^2 value of .992 (excluding beam AW-2) whereas the flush-ground beams had an R^2 value of .826.

4.1.4 Effect of Edge Notches

Although not explicitly part of the test program, two beams (GF-7 and GF-8) had notches at the flange tips and subsequently showed significantly different types of failure and fatigue lives than the equivalent beams without these edge notches.

The notches were readily visible in the fabricated beams, as shown in Fig. 4.7. They were approximately 1/8 in. long and 1/16 in. deep. The fatigue crack initiated at these notches and grew at a substantially faster rate than the cracks that initiated in the flange-to-web fillet welds. In beam GF-7, failure occurred at less than one-half the number of cycles of an equivalent beam without a notch (GF-9) tested at the same stress range.

In several other beams which had notches in the flange tip, an attempt was made to improve the fatigue strength by grinding the notches. The tip of the flange was ground at the notch and in the surrounding area in order to give a gradual transition in flange width and thus remove the abrupt stress concentration. From tests on these beams it was observed that the notches, after grinding, had no apparent effect on the fatigue life. In all cases, the resulting fatigue crack causing failure occurred away from the notched area and at a number of cycles comparable to an unnotched beam tested at the same stress range. The failure cracks in these cases initiated at the flange-to-web fillet weld.

4.1.5 Effect of Weld Flaws

The failure cracks which initiated in the flange-to-web fillet welds originated at a flaw in the weld itself. These flaws were in the form of porosity, slag inclusions, poor fit-up, lack of penetration or a combination of these.

Often the porosity or gas pockets were quite large and were visible without significant magnification. Figures 4.8 and 4.9 show two specimens (Beams GF-4 and AW-3, respectively) where fatigue cracks grew from pores in the fillet weld. These were typical of the flaw sizes observed, and resulted in fatigue lives close to the mean regression line for plain-welded beams, as obtained by Fisher et al (2).

The cracks starting at these flaws grew outward in a circular pattern as shown in Fig. 4.10. A significant portion of the fatigue life was spent propagating the crack through the weld to the surface. For the particular specimen shown, (Beam AW-1), approximately 95% of the fatigue life was exhausted in forming the circular, discoloured crack area shown in the figure.

In several of the beams, cracking originated from slag inclusions in the fillet weld. Figures 4.11(a) to 4.11(d) show successive magnifications of the crack initiation region, taken by means of optical and electron scanning microscopes, for Beam GF-4. A chemical analysis of the oval shaped area in Fig. 4.11(d) revealed a predominance of silicon, calcium, and potassium. This would indicate trapped slag from the welding process. Fisher et al. found that the majority of the fatigue cracks of this type originated in the vicinity of tack welds or weld repairs (2). In this case the flaw was quite small and resulted in a fatigue life greater than the mean for plain-welded beams.

Figures 4.12(a) and (b) show specimen number GF-2 which had a particularly poor fillet weld. This specimen had several of the previously described flaws in the weld. There was poor fit-up between web and flange, slag inclusions and gas pockets in the weld, and also a slight undercut at the weld toe. As a result of these serious flaws, the fatigue strength of this beam was significantly lower than other beams tested at this stress

range. It should be noted that a visual inspection of the fillet weld, prior to testing, revealed none of these flaws. More sophisticated inspection techniques were not used for the fillet welds as standard practice would not normally require such inspection procedures for this type of weld.

The failure crack originating in the specimen with an undercut in the groove weld resulted in a considerable fatigue strength reduction (Beam AW-2). The undercut occurred in an area of a splice on the main source plate prior to cutting the flanges to width. The X-ray inspection detected this flaw and the fabricator was then instructed to repair the weld, or to trim and waste that particular area of plate. Unfortunately, a follow-up X-ray inspection was not performed after the repair and a portion of the undercut still remained.

The seriousness of this type of welding flaw is emphasized by the magnitude of the fatigue life which was obtained in the test. The number of cycles to failure was approximately one million, whereas the two other beams of this type, tested at the same stress range, failed at five million cycles.

4.1.6 Comparison with Previous Studies

The majority of the beams tested with the weld reinforcement ground flush had fatigue strengths close to the mean regression line for plain-welded beams, as obtained in the Lehigh and Drexel test series (2). Figure 4.13 shows the mean

regression line and the upper and lower limits of dispersion from that test series. The lower dashed line is also the 95% confidence limit for 95% survival. The broken line is the mean regression line calculated using results of the nine beams tested in this series with flush-ground groove welds.

It can be seen that two points fall on or slightly below the 95% confidence limit for 95% survival (Specimens GF-2 and GF-7). The point at the high stress range was the beam which failed from a crack initiating at a notch in the flange tip (GF-7), while that at the low stress range was the beam with the major fillet weld flaw (GF-2).

The current method for fatigue design according to AASHTO (4) and CSA (5,6) specifications would be to classify the flush-ground groove-welded beams as stress category B. This category is based on the 95% - 95% line for plain-welded beams as obtained in the Lehigh and Drexel tests and as shown in Fig. 4.13.

The classification of flush-ground groove welds as category B would appear to be a suitable choice in light of the results of this test series. All of the beams had fatigue strengths very close to, or above, the allowable stress range for this particular category.

Eight of the nine beams tested with as-welded groove welds had fatigue strengths between the 95% - 95% line and the mean regression line for plain-welded beams. Figure 4.14 shows the mean line for these test results as well as the mean regression

line and dispersion limits obtained in the Lehigh and Drexel tests for plain-welded beams (2).

It can be seen that one point (Beam AW-2) falls significantly below the 95% confidence limit for 95% survival. As noted earlier, this was the beam which failed from a crack initiating in the groove weld undercut.

AASHTO and CSA specifications would presently classify beams with as-welded groove welds as stress category C. This category is based on the 95% - 95% limit for beams with 2 in. welded flange attachments (3) which is shown as the lower line in Fig. 4.14. Specific tests on as-welded beam details were not carried out in the Lehigh and Drexel investigations and thus this classification was a matter of judgement.

As can be seen from the test results in Fig. 4.14, the classification of as-welded beams as category C would appear to be conservative. Eight of the nine beams had fatigue strengths above that allowed for category B and only Beam AW-2, which failed from a major groove-weld flaw, had a fatigue strength near the category C line.

It is important to note that both categories B and C specify that the weld soundness of the groove welds be established by non-destructive inspection. A complete inspection should have detected the groove weld undercut in Beam AW-2 prior to testing, and an adequate repair should have been carried out. The test results indicate the extreme importance of this procedure.

4.2 Phase 2 (Beams with Lateral Bracing Attachments)

4.2.1 Crack Initiation and Growth

All of the beams tested in this phase of the program failed in the same manner. The fatigue cracks occurred at the fillet weld toes at either end of the gusset plate attachment. The cracks then grew vertically, both upward and downward in the beam web, and eventually through to the opposite side of the web. Figure 4.15 shows a typical failure crack. The cracks propagated from the weld toe in a semi-elliptical shape through the thickness of the web. This crack shape is shown in Fig. 4.16.

Failure of the section was considered complete, and the testing stopped, when the fatigue crack had grown entirely through the web thickness. At this point, the cracks were normally in the range of 1 in. to 1-1/2 in. long. Crack growth was quite rapid at this stage as approximately 98% of the fatigue life was exhausted in propagating the crack through the web thickness.

Upon reaching the failure criterion, the fatigue crack was repaired and the testing resumed. (The method of crack repair was described in Section 3.3.3). The weld repairs were generally successful, in that four fatigue cracks (one at each end of the two gusset plates) were obtained in most of the beams, prior to recracking of the weld repair. Of the seven beams of this type which were tested, 24 out of a possible 28 fatigue cracks were obtained.

There were no other cracks observed in any other regions of the beam, the stiffener, or the horizontal gusset plate.

4.2.2 Effect of Stress Range

As expected, stress range had a significant effect on the fatigue life. As in Phase 1, the minimum stress was maintained at a constant value and only the stress range was varied. It was found that the fatigue life decreased as the stress range increased.

Figure 4.17 summarizes the test data for the seven beams which were tested. Each data point represents a separate fatigue crack, although many were in beams which were retested after weld repairs. Table 4.2 gives a complete summary of the test series. A linear regression analysis was carried out on the test data using the model $\text{Log } N = B_1 + B_2 \text{ Log } Sr$. The solid line in Fig. 4.17 represents the mean regression line.

In the beam tested at the 9 ksi stress range (Beam L-6), only one fatigue crack occurred. No other cracks were observed in the other three probable locations (at the ends of the two gusset plate attachments), although the beam was subjected to over six million cycles of loading. This stress range was probably very close to the fatigue limit for this type of detail and material.

4.2.3 Effect of Lateral Bracing

The presence of lateral bracing as provided for in these specimens had no observable effect on the fatigue lives of the test beams. The cracks which formed at the fillet weld toes, at either end of the gusset plate attachment, occurred randomly at each of the four locations in the beams. It appears that the gusset plate detail alone was the major influencing factor, not the detail in combination with the lateral bracing.

The shape of the fillet weld toe appeared to have an effect on the fatigue life. In the locations where the toe of the fillet weld at the gusset plate-beam web junction was fairly abrupt, the fatigue life was slightly less than where the weld had a more tapered transition. This was probably due to the higher stress concentration at the abrupt fillet weld toe. However, all of the fillet welds used for these details would be acceptable for standard construction practice, and this effect on the fatigue life was relatively minor.

Within the limits of the test parameters, the various sizes of gusset plates, bracing angles and bracing lengths had no observable effect on the fatigue strength. The variations included gusset plates of 5/16 in and 3/8 in. thicknesses, bracing angles of 1/4 in. and 3/8 in. thicknesses and bracing lengths of 25 in. and 70 in. In order to establish suitable criteria for the bracing, a survey was conducted on two steel bridges in the Edmonton area. This survey involved a measurement

of the girder deflections under heavy truck loading and also a recording of the lateral and transverse bracing stiffnesses. (This survey is described in detail in Appendix A.) It was found that the maximum rotations induced in the bracing members of the two bridges under heavy truck loadings were both approximately 0.04 degrees. In this test program the rotation angles ranged from 0.12 to 0.21 degrees, depending on the maximum stress applied and the lengths of the bracing members. The stiffnesses of the bracing members in the two bridges surveyed were calculated as the sum of $3EI/L^3$ for each bracing member framing into the attachment detail. These stiffness values were found to be 0.14 k/in. and 0.19 k/in. For this test program the stiffnesses of bracing members were 7.61 k/in. for specimen L-1 and 0.29 k/in. for the remaining six specimens. As a result of these measurements, it was felt that the experimental set-up gave a good approximation to actual bridge girder deflections and bracing stiffnesses. Any variations from an actual bridge were on the conservative side as the bracing used for the tests tended to be slightly stiffer than that of the two bridges investigated.

4.2.4 Stress Distribution in Attachments

Fisher et al. showed that the amount of load carried by the attachment plates varies with their length along the beam (3). Using a finite element analysis, they found that the attachment will develop its full capacity if its length

along the beam is at least equal to three to four times its width. These studies were carried out on beams with attachments welded to the tension flange.

In the tests reported herein, strain gauges were mounted on the gusset plates and static load tests were carried out to determine the stress distribution. Figure 4.18 shows the locations of these strain gauges. On the gusset plates without lateral bracing attached, the gauges were mounted in an attempt to measure the stress distribution in the gusset, adjacent to the vertical stiffener. These gauges were all oriented to measure strains in the longitudinal direction of the beam. All were located 1-1/2 in. from the centre of the stiffener. One gauge was located on the beam web at the level of the gusset plate, and the remaining gauges were at distances of 3/4, 1-1/2, 2-1/4, and 3 in. from the beam web, on the gusset plate itself.

On the gusset plates with the attached lateral bracing, the strain gauges were mounted in an attempt to measure the stresses in the gusset due to the forces transferred from the bracing members. As shown in Fig. 4.18, one gauge was located on the gusset in a transverse direction to the centre-line of the beam, near the end of the plate at the beam web. A second gauge was positioned on the gusset in a direction parallel to the beam centre-line, near the outside end of the stiffener.

The experimentally determined stress distribution in the gusset plate without bracing members is shown in Fig. 4.19.

These stresses are the average values obtained for all the static load tests on the members under maximum load. The maximum load produced a stress of 32 ksi at the extreme fibre of the beam and a midspan beam deflection of about 1/4 in. The results indicate that there are fairly large stresses in the gusset plate, but the stresses reduce very quickly as the perpendicular distance from the beam web increases. The stress in the plate is almost zero near the end of the vertical stiffener.

In the gusset plate with lateral bracing members attached, the strain gauge readings indicate that there is a substantial stress created by the transfer of forces from the bracing. Under maximum static load, stresses of between 10 ksi and 12 ksi were measured in both gauges 6 and 7. The majority of this must have been a result of the bracing member forces since the strain gauge in a similar location on the gusset plate without bracing members (gauge 5) indicated almost zero stress near the end of the stiffener. Test measurements taken on the Conestogo River Bridge in Ontario revealed stresses of from 10.0 ksi to 12.8 ksi in the bottom lateral bracing connections of a similar detail under static loading conditions (23,24).

These static load tests have thus shown that a considerable amount of load is carried by the lateral gusset plates. This is basically due to two loading effects. One is the force developed due to flexure of the beam, which is transferred by means of shear in the fillet weld from the beam web to the gusset

plate. The other effect is the secondary stresses which develop in the gusset due to the forces transferred from the lateral bracing members. These forces can result from the differential vertical deflections of the beams and will be both transverse and parallel to the beam axis. Although the latter stresses were shown to be of significant magnitude, the tests revealed that these secondary bending stresses had no observable effect on the fatigue strength of the beam. It would appear that the flexural stress in the web, at the level of the gusset plate, governs the fatigue life of this type of detail.

4.2.5 Comparison with Previous Studies

The majority of the beams tested in this phase of the program had fatigue strengths close to, or above, the mean regression line for beams with end-welded cover plates, as obtained in the Lehigh and Drexel test series (2). Figure 4.20 shows the mean regression line and the upper and lower limits of dispersion from the test series. The lower dashed line is also the 95% confidence limit for 95% survival which is the basis for stress category E according to AASHTO and CSA (4,5,6). The broken line is the mean regression line for the 24 fatigue cracks from this test series. All the beams had fatigue lives above the 95% - 95% line for end welded cover-plated beams.

In the Lehigh and Drexel programs beams were tested with attachments fillet-welded to the tension flanges (2,3).

The longest attachment tested was 8 in. It was observed that the beams with 8 in. attachments had only slightly higher fatigue strengths than beams with end-welded cover plates.

As a result of the Lehigh and Drexel tests, the AASHTO and CSA specifications classify fillet-welded rectangular attachments as stress category C, D, or E, depending on their lengths (3,4,5). If the detail length in the direction of stress is less than 2 in., then it is category C; if it is between 2 in. and 12 times the plate thickness, but less than 4 in., then it is category D; and if it is greater than 12 times the plate thickness, or greater than 4 in., then it is category E. Thus, the 8 in. attachment details, tested in the Lehigh and Drexel tests, and the 10 in. details, tested in this program, would both be in category E.

The classification of the 10 in. attachments in this test program as category E would appear to be reasonable as indicated by the test results. All of the beams had fatigue strengths above the allowable stress range for this particular category.

TABLE 4.1 SUMMARY OF TEST RESULTS

PHASE 1

Specimen	Sr Stress Range (ksi)	First Observed Crack ($\times 10^3$)	N Failure ($\times 10^3$)	Failure Crack Initiation
GF-1	17	-	6,295.5	F
GF-2	17	-	2,251.5	F
GF-3	17	-	5,382.0	F
GF-4	25	1,930.5	1,974.0	F
GF-5	25	1,422.0	1,446.0	F
GF-6	25	-	1,735.5	F
GF-7	32	-	300.0	N
GF-8	32	-	537.0	N
GF-9	32	-	748.5	F
AW-1	17	4,806.0	4,972.5	F
AW-2	17	-	993.0	U
AW-3	17	-	5,100.0	F
AW-4	25	-	1,051.5	R
AW-5	25	-	1,084.5	R
AW-6	25	-	855.0	R
AW-7	32	-	424.5	R
AW-8	32	-	339.0	R
AW-9	32	-	343.5	R

In all cases, σ_{min} = 8 ksi

GF = Groove weld ground flush
AW = As-welded groove weld
F = Flaw in flange-to-web fillet weld
N = Notch in flange tip
R = Toe of groove weld reinforcement
U = Undercut in groove weld

TABLE 4.2 SUMMARY OF TEST RESULTS

PHASE 2

Specimen	Gusset Thickness (inches)	Bracing Attached	Bracing Length (inches)	Sr At Attachment (ksi)	First Observed Crack ($\times 10^3$)	N Failure ($\times 10^3$)
L-1	3/8	NO	-	19.5	-	214.5
	3/8	NO	-	19.5	-	259.5
	3/8	YES	25	15.9	-	370.5
	3/8	YES	25	15.9	-	400.5
L-2	5/16	NO	-	19.5	-	156.0
	5/16	YES	70	19.5	-	156.0
	5/16	NO	-	19.5	-	172.5
	5/16	YES	70	19.5	-	250.5
L-3	5/16	YES	70	17.0	-	469.5
	5/16	NO	-	17.0	469.5	511.5
	5/16	YES	70	17.0	574.5	625.5
	5/16	NO	-	17.0	616.5	640.0
L-4	5/16	NO	-	13.0	-	517.5
	5/16	NO	-	13.0	517.5	628.5
	5/16	YES	70	13.0	-	825.0
	5/16	YES	70	13.0	933.0	1,020.0
L-5	5/16	NO	-	13.0	895.5	955.5
	5/16	YES	70	13.0	-	985.5
	5/16	YES	70	13.0	1,288.5	1,306.5
	5/16	NO	-	13.0	1,306.5	1,438.5
L-6	5/16	YES	70	9.0	2,397.0	2,735.0
	5/16	YES	70	9.0	-	6,639.0*
	5/16	NO	-	9.0	-	6,639.0*
	5/16	NO	-	9.0	-	6,639.0*
L-7	5/16	NO	-	11.0	1,254.0	1,473.0
	5/16	NO	-	11.0	1,353.0	1,696.5
	5/16	YES	70	11.0	1,464.0	1,696.5
	5/16	YES	70	11.0	-	2,406.0*

* = Test discontinued before crack observed.

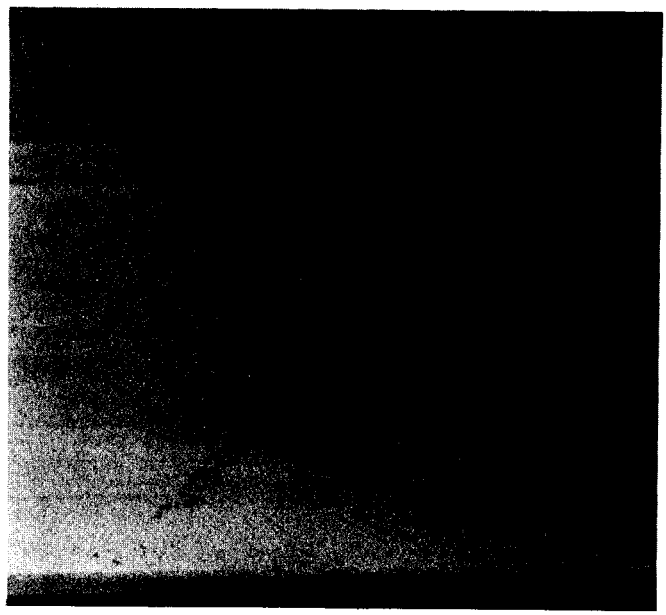

FIGURE 4.1(a) CRACK IN FLANGE-TO-WEB FILLET WELD

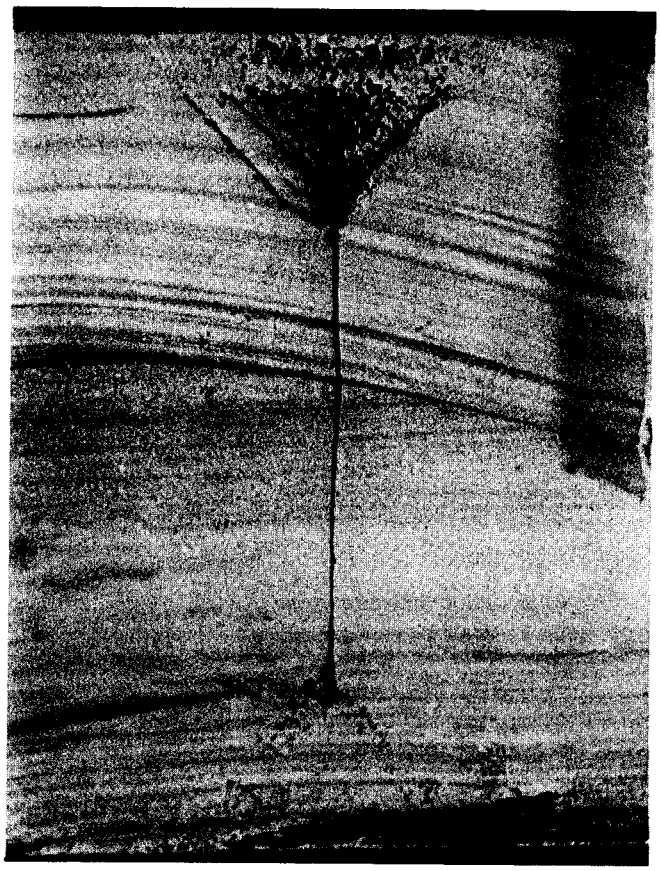

FIGURE 4.1(b) CRACK IN FLANGE-TO-WEB FILLET WELD
(UNDERSIDE OF BEAM)

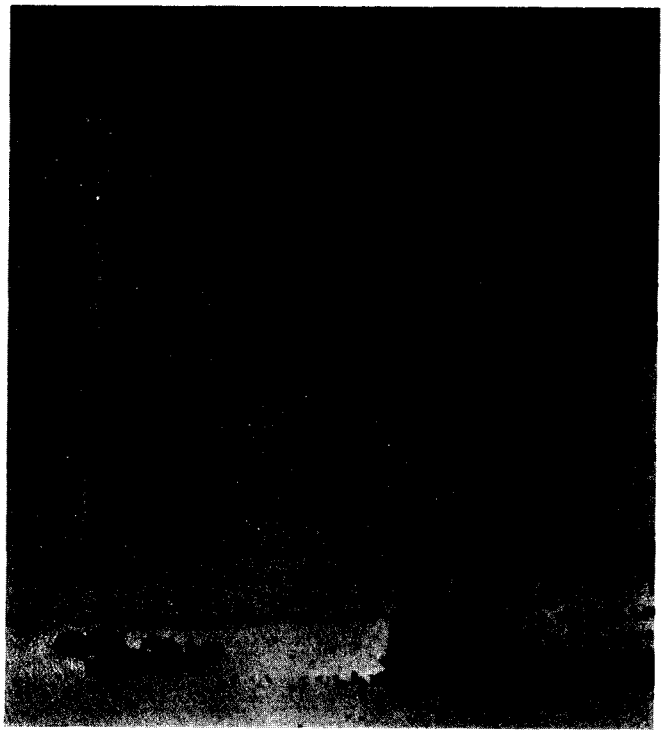

FIGURE 4.2 CRACK INITIATING AT NOTCH IN FLANGE TIP

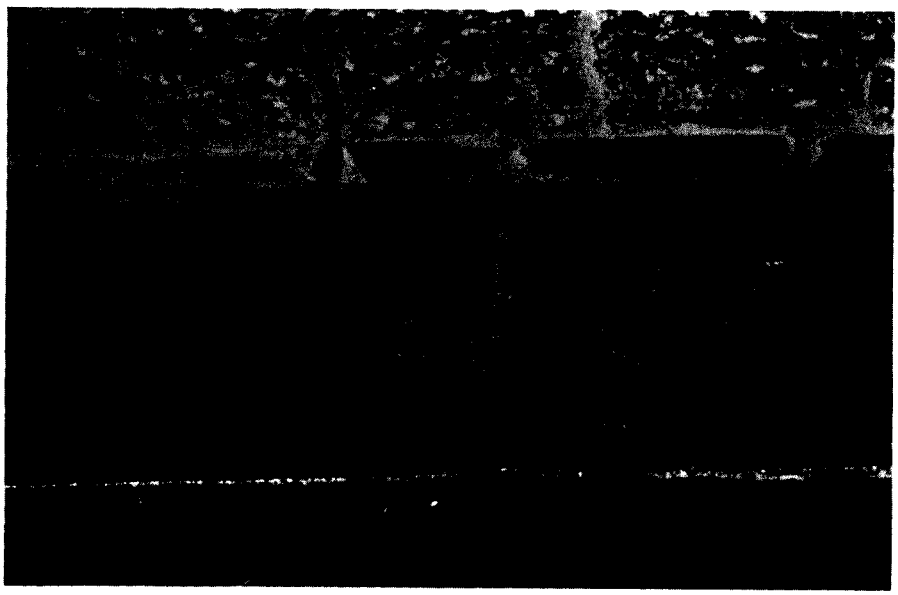

FIGURE 4.3 CRACK INITIATING AT TOE OF GROOVE WELD REINFORCEMENT

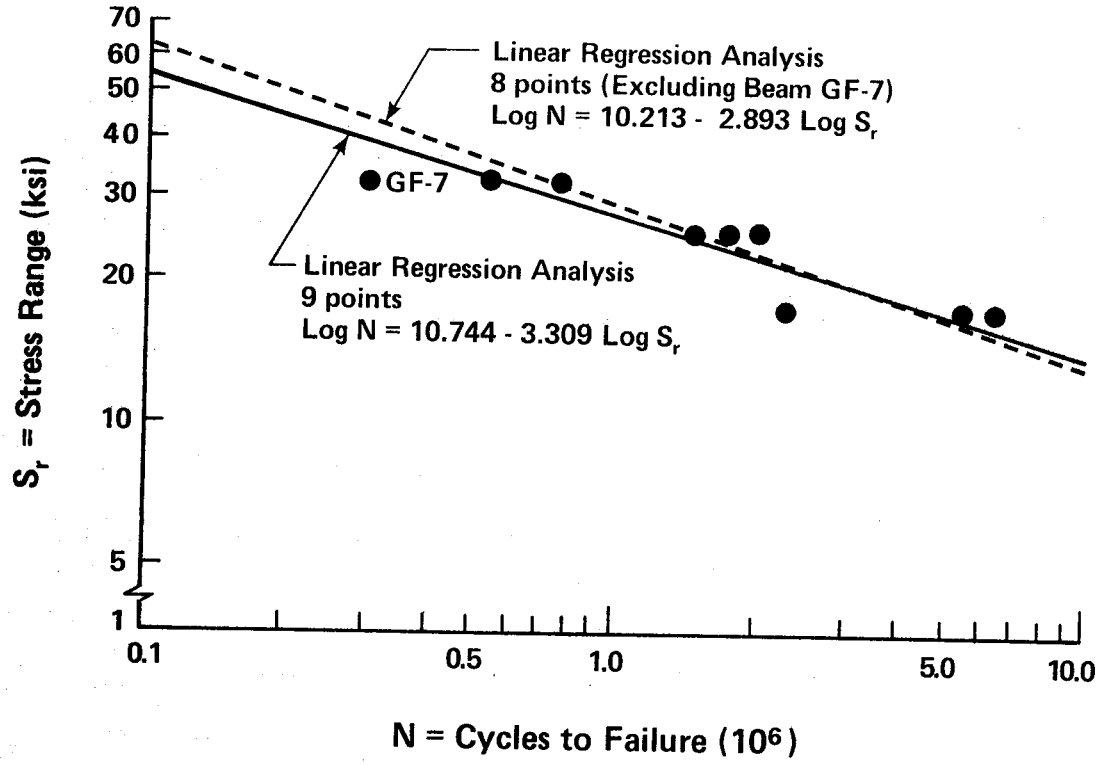

FIGURE 4.4 BEAMS WITH GROOVE WELD REINFORCEMENT GROUND FLUSH

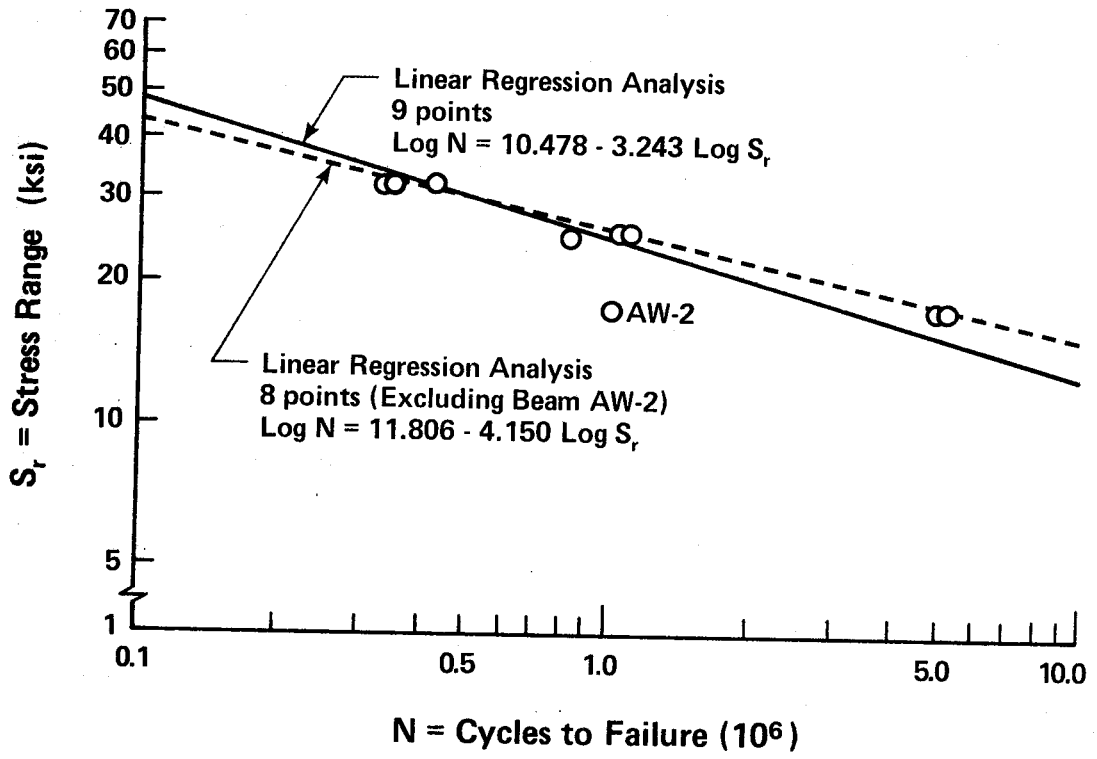

FIGURE 4.5 BEAMS WITH GROOVE WELD REINFORCEMENT AS-WELDED

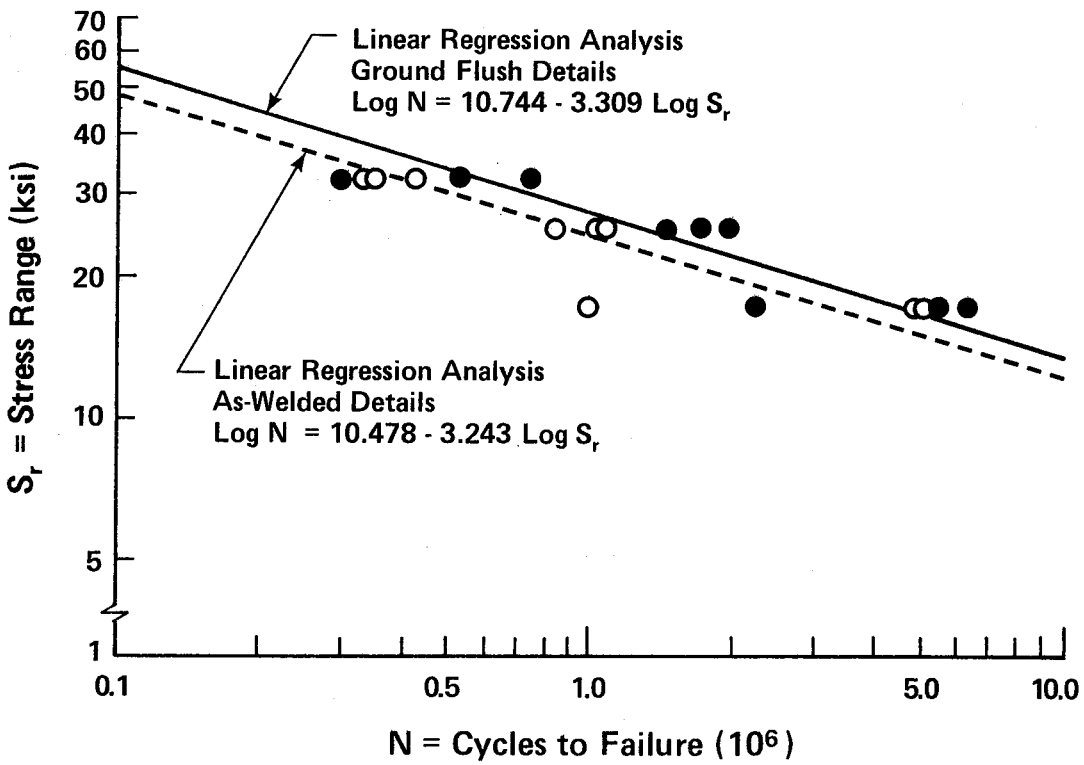

FIGURE 4.6 BEAMS WITH GROOVE-WELDED FLANGE PLATES

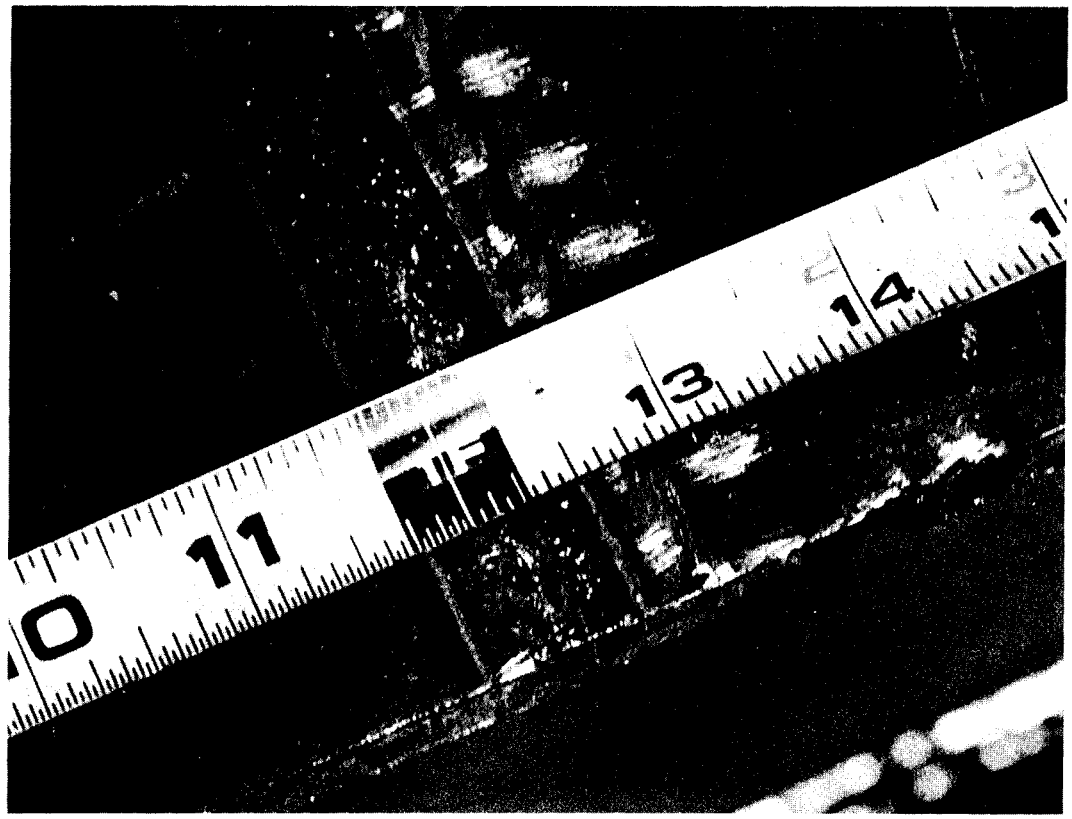

FIGURE 4.7 EDGE NOTCH IN FLANGE TIP

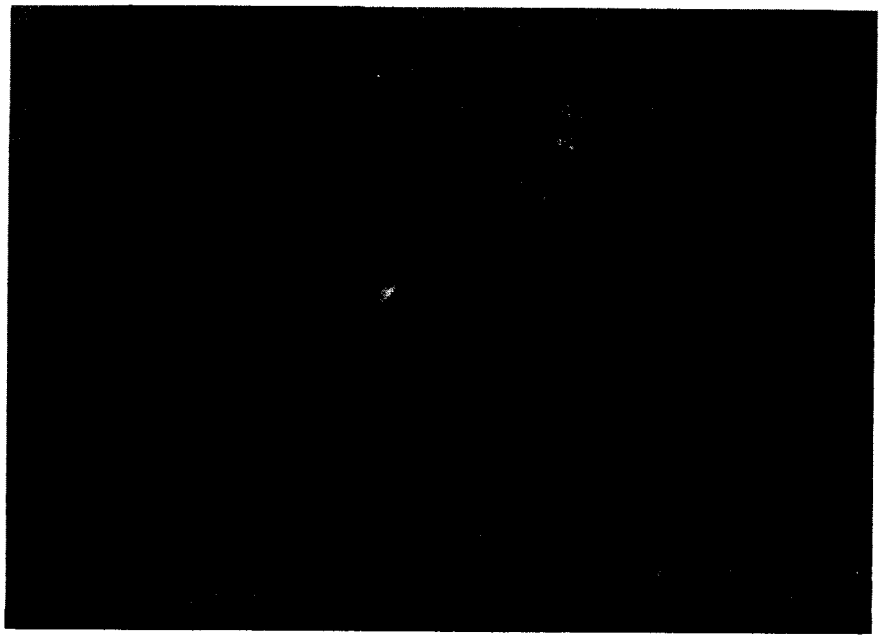

FIGURE 4.8 FLANGE-TO-WEB FILLET WELD FLAW

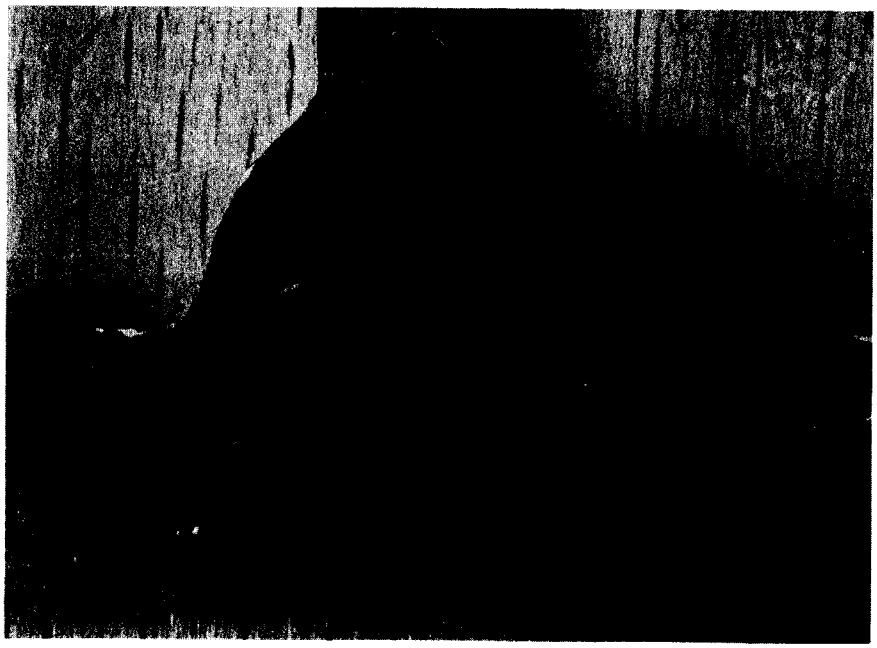

FIGURE 4.9 FILLET WELD FLAW

FIGURE 4.10 FILLET WELD FLAW AND FATIGUE CRACK

FIGURE 4.11(a) FATIGUE CRACK (X3.5)

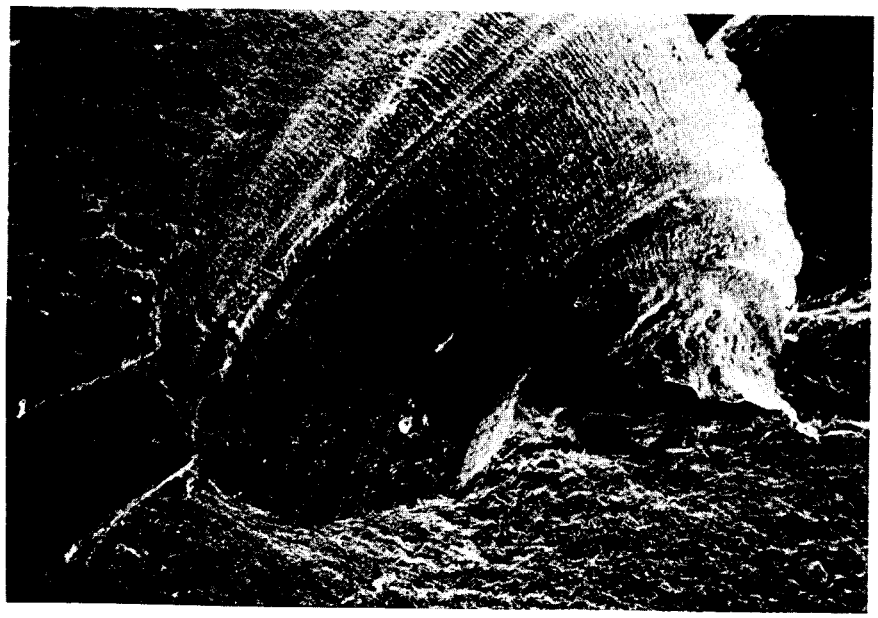

FIGURE 4.11(b) FATIGUE CRACK (X52)

FIGURE 4.11(c) FATIGUE CRACK (X200)

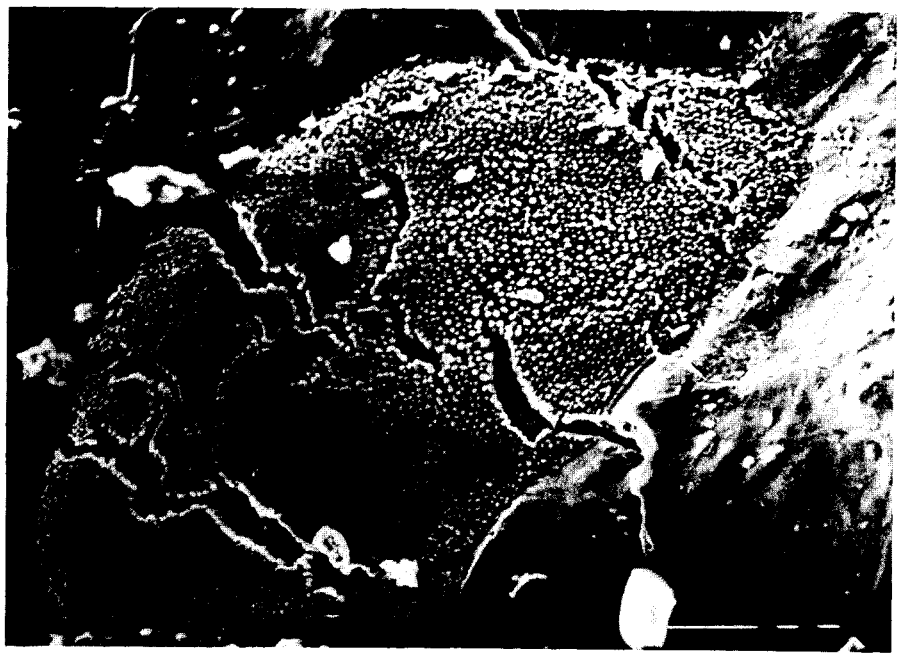

FIGURE 4.11(d) FATIGUE CRACK (X1000)

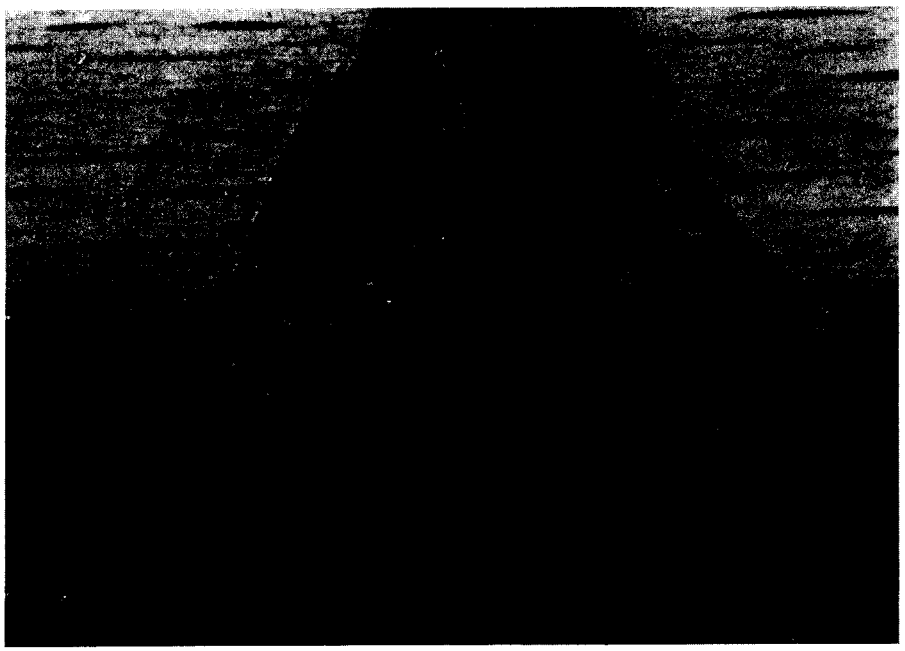

FIGURE 4.12(a) FILLET WELD FLAW (X3.5)

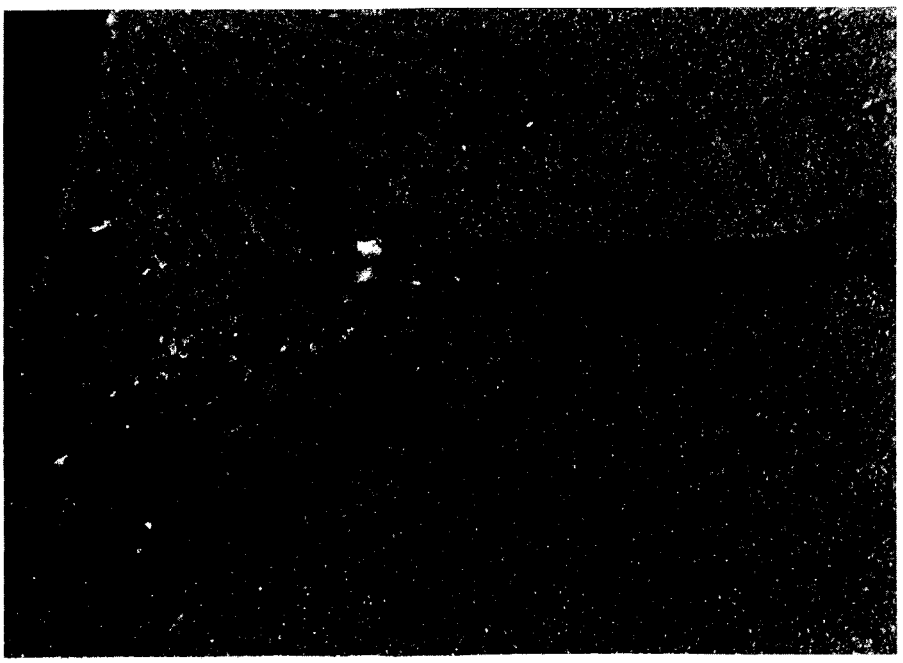

FIGURE 4.12(b) FILLET WELD FLAW (X8.75)

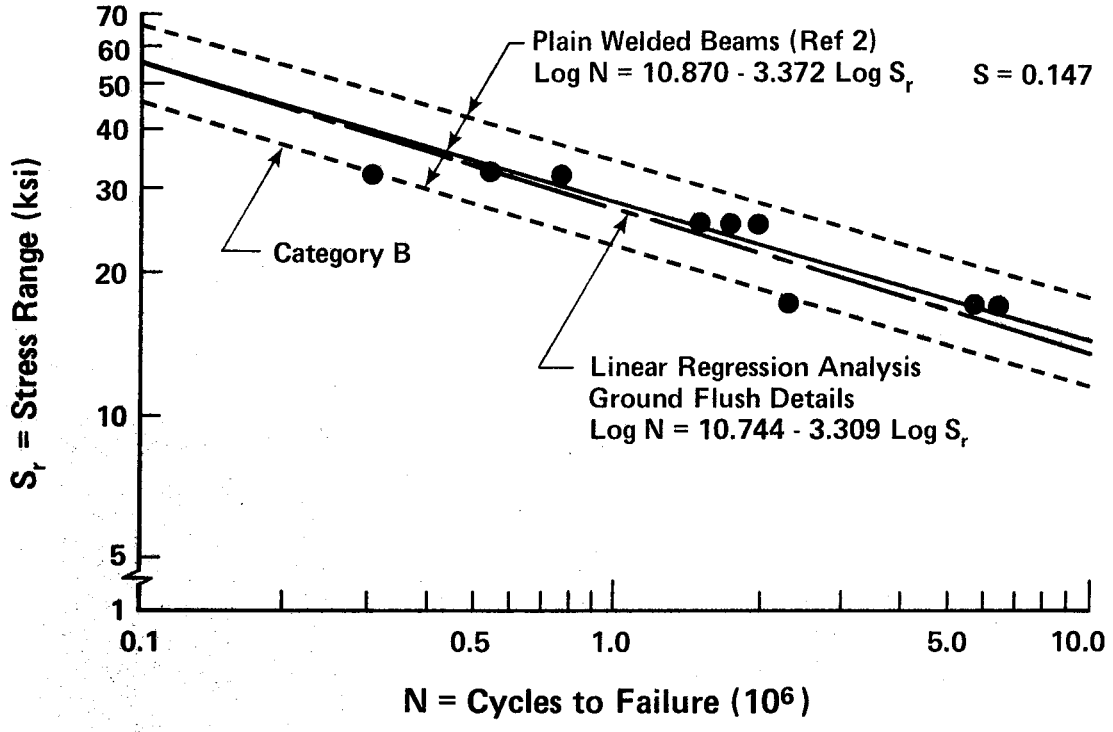

FIGURE 4.13 PLAIN WELDED BEAMS AND FLUSH GROUND GROOVE-WELDED BEAMS

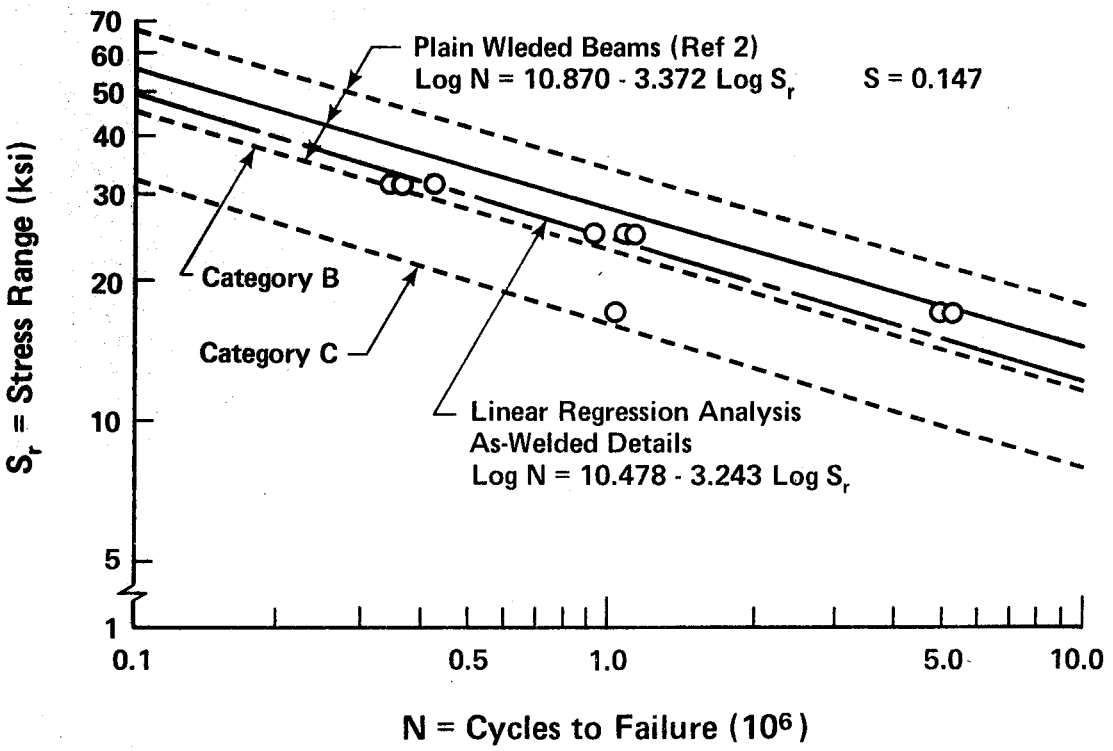

FIGURE 4.14 PLAIN WELDED BEAMS AND AS-WELDED GROOVE-WELDED BEAMS

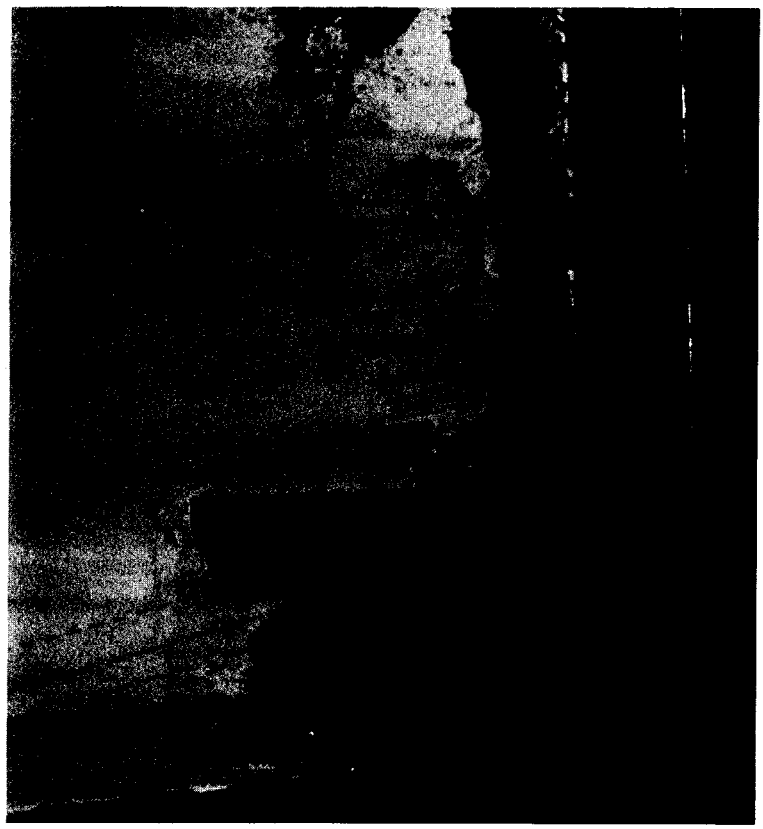

FIGURE 4.15 FATIGUE CRACK AT END OF GUSSET PLATE ATTACHMENT

FIGURE 4.16 FATIGUE CRACK IN BEAM WEB AT TOE OF GUSSET PLATE FILLET WELD (X3.25)

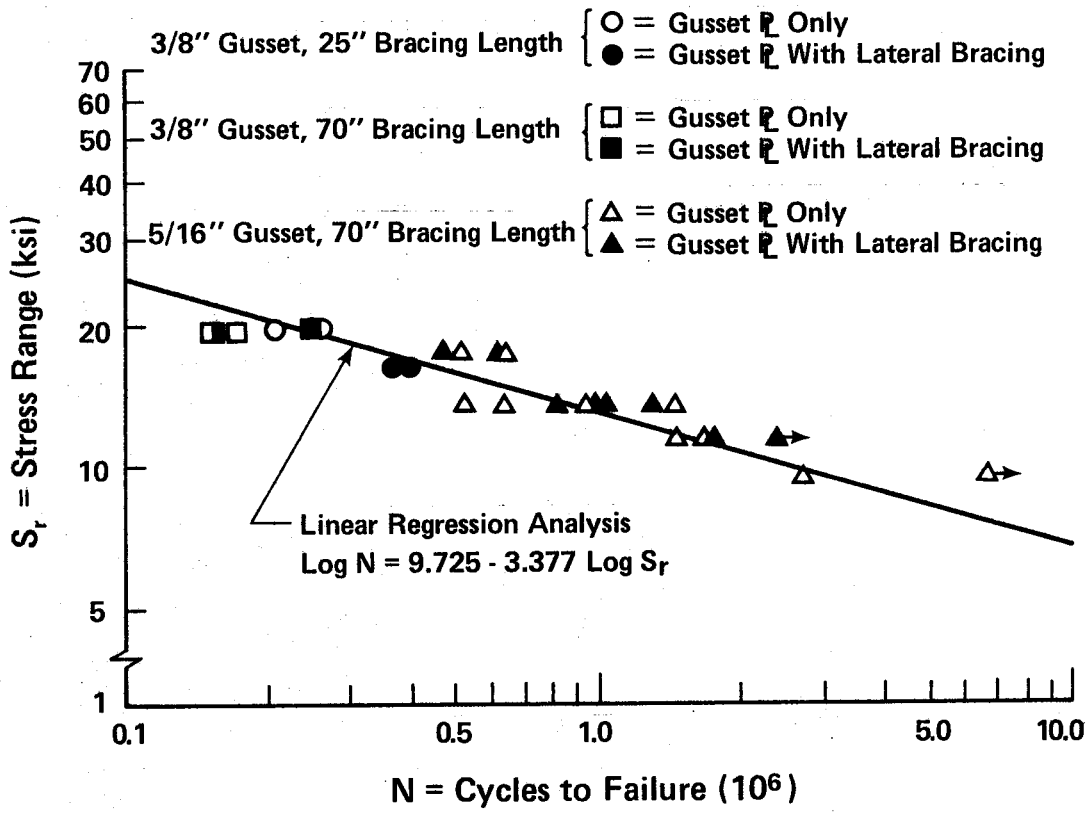

FIGURE 4.17 BEAMS WITH LATERAL BRACING ATTACHMENTS

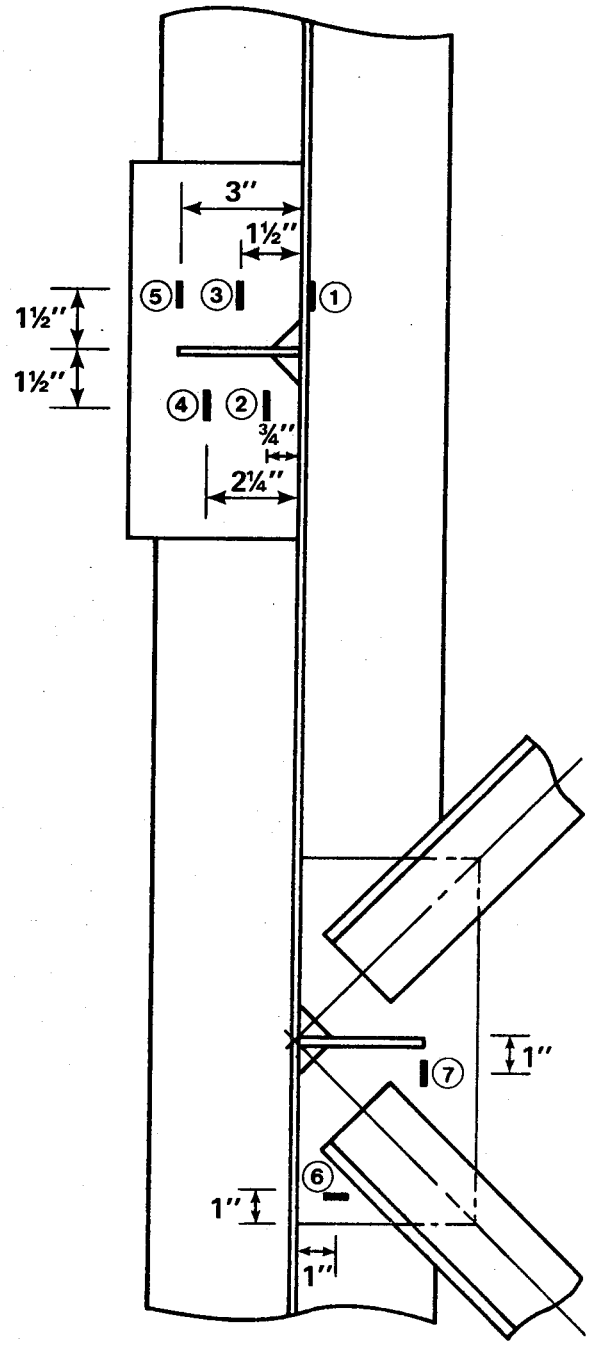

FIGURE 4.18 STRAIN GAUGE LOCATIONS ON LATERAL GUSSET PLATES

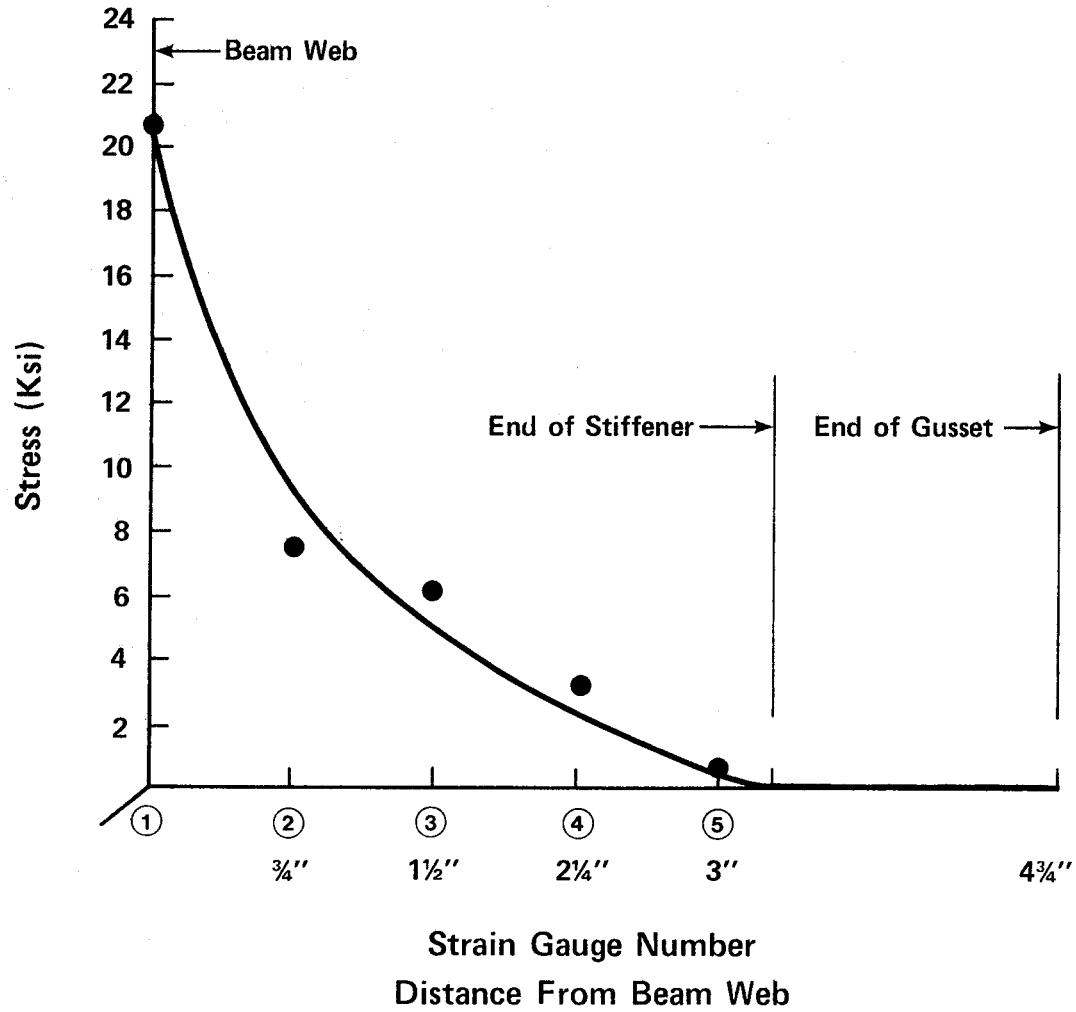

FIGURE 4.19 STRESS DISTRIBUTION IN GUSSET PLATE WITHOUT BRACING ATTACHED

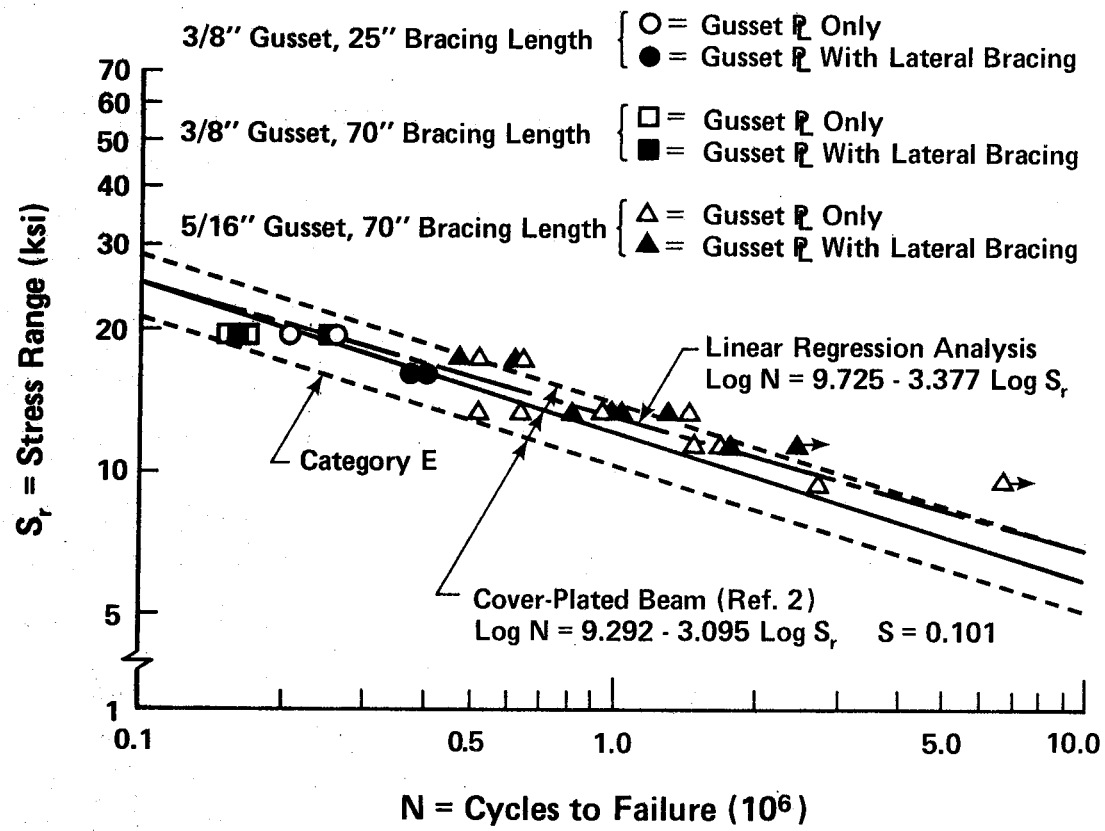

FIGURE 4.20 BEAMS WITH END-WELDED COVER PLATES AND BEAMS WITH LATERAL BRACING ATTACHMENTS

CHAPTER V

FRACTURE ANALYSIS OF TEST SPECIMENS

5.1 Introduction to the Analysis

In this chapter a fracture mechanics approach will be used to predict the fatigue lives of the test specimens. These predictions will then be compared with the test results. All of the four major types of fatigue cracks which caused failure in the test beams will be discussed. These include cracks which initiated at internal flaws in the flange-to-web fillet welds, those which initiated at a notch in the flange tip, those which initiated at the toe of the groove weld reinforcement, and those which initiated at the ends of the bracing attachment details. Prior to the analysis of the specific crack types, a review of the fracture mechanics method of analysis of crack growth will be presented. This includes a derivation of the log-linear model used in the regression analysis of Chapter IV.

At the conclusion of this chapter an analysis will be conducted which relates the groove weld reinforcement angle to the fatigue strength. This includes a discussion of past investigations into this effect and its use in predicting the test results of this study.

5.2 General Background on Crack Growth

There are three stages in the fatigue life of a structural member. These stages are, in order of occurrence, initiation of the fatigue crack, fatigue crack propagation, and fracture.

The crack initiation stage is generally not a concern in the prediction of the fatigue life of a structural component. Studies have shown that the majority of steel structural components contain initial discontinuities or defects from the manufacturing and/or fabricating processes (28). These defects range from micro-flaws in welds to notches in flame cut edges. Although most of these discontinuities will not be visible to the observer, they are sufficient in size to constitute the initiation of a fatigue crack. Thus, this stage in the fatigue life of the component has already occurred, and consequently the analysis is concerned with determining the size of this initial flaw rather than when, or if, it will occur.

The final stage, fracture, is again not a major concern in predicting fatigue life. Prior to reaching this stage, the useful life of the structural component will have been essentially exhausted. By the time the fatigue crack is of sufficient size to precipitate failure by some other mode, such as general yielding or brittle fracture, then the crack will be growing at a very rapid rate. This would make accurate prediction of the fracture stage both difficult and unnecessary. Thus, in

prediction of fatigue life, the basic concern is the estimation of the second stage, that of fatigue crack propagation.

The presently accepted approach is that fatigue crack propagation is dependent on plastic deformation at the crack tip or notch (13,14,15). This is a localized plastic flow due to the high stress concentration in this region. The plastic deformation causes a shearing slip on a crystallographic plane and thus the crack grows by a series of slip bands caused by repeated applications of stress. Although the yield strength, tensile strength, and strain-hardening properties of the material have been shown to have an effect on the crack initiation stage (14), tests have revealed that they have essentially no effect on the crack propagation stage (2,13,14). These studies have indicated that the major factors influencing fatigue crack propagation are the nominal stress range acting at the section, initial notch size, and the stress concentration factor.

The crack propagation stage can be represented by the semi-empirical equation of crack growth developed by Paris (21),

$$\frac{da}{dN} = C(\Delta K)^n \qquad (5.1)$$

where a = crack length,

N = number of cycles,

ΔK = stress range intensity factor,

n = constant,

C = constant of proportionality of crack growth.

The stress range intensity factor, ΔK, accounts for the stress field in the vicinity of the crack tip. It is dependent upon the crack size, geometry, and nominal stress range. Irwin has determined that the general form of the stress-intensity factor is as follows (22):

$$K = f(g)\ \sigma \sqrt{a} \tag{5.2}$$

where σ = applied nominal stress,

$f(g)$ = parameter depending on the specimen and crack geometry.

The term $f(g)$ has been investigated in great detail and values are available for a variety of cases (14).

Equation 5.2 can be substituted into Eq. 5.1 and the result integrated between the limits of crack size at initiation, a_i, and at failure, a_f, in order to determine the number of stress cycles to failure. These steps are:

$$\frac{da}{dN} = C[f(g)\ \Delta\sigma \sqrt{a}\,]^n \tag{5.3}$$

Substituting S_r for the change in nominal stress $\Delta\sigma$, and integrating gives:

$$\Delta N = \int_{a_i}^{a_f} (C^{-1}\ f(g)^{-n}\ S_r^{-n}\ a^{-n/2})da$$

$$= \left[\frac{1}{C}\ f(g)^{-n}\ S_r^{-n}\ \frac{a^{1-\frac{n}{2}}}{(1-\frac{n}{2})}\right]_{a_i}^{a_f}$$

Letting m = n/2 - 1 gives

$$\Delta N = \frac{1}{C} f(g)^{-n} S_r^{-n} \frac{1}{m} (a_i^{-m} - a_f^{-m}) \tag{5.4}$$

This development assumes that f(g) is independent of an increase in crack size. This will be the case until the crack becomes quite large in size.

The final crack size is generally very large in comparison to the initial crack size. The term a_f can therefore be disregarded as it will have little effect on the cycle life. Equation 5.4 can thus be simplified to:

$$\Delta N = \left[\frac{1}{C} f(g)^{-n} \frac{1}{m} a_i^{-m} \right] S_r^{-n} \tag{5.5}$$

The quantity in parenthesis will be constant for a given material, geometry, and initial crack size. Letting M represent this quantity,

$$\Delta N = M S_r^{-n} \tag{5.6}$$

Expressed in logarithmic form, this will be:

$$\text{Log } N = \text{Log } M - n \text{ Log } S_r \tag{5.7}$$

Substituting B_1 for Log M and B_2 for (-n) results in the same equation that was used for the linear model in

the regression analysis of Chapter IV. That is:

$$\text{Log } N = B_1 + B_2 \text{ Log } S_r \qquad (5.8)$$

5.3 Fracture Mechanics Analysis

5.3.1 Cracks Initiating in Fillet Welds

The fillet weld cracks can be analysed by assuming that the crack grows in a circular shape from the internal weld flaw. This was found by Fisher et al. to be the case until the crack penetrated the outside surface of the flange (2). Rolfe gives the correction factor f(g), for a circular crack in an infinite plate as $(2.0/\sqrt{\pi})$ (14). This results in a value of K equal to $(2.0/\sqrt{\pi})\ \sigma\ \sqrt{a}$. Fisher found this value to give good correlation with test results.

The value of C, the constant of proportionality of crack growth, is essentially a function of the microstructure of the steel. Rolfe and Barsom (14) found that ferrite-pearlite steels have lower fatigue crack growth rates than martensitic steels. They attribute this lower growth rate to the stronger pearlite colonies in the ferrite-pearlite matrix, which cause secondary fatigue cracks and crack branching, consequently retarding crack growth.

Rolfe gives, as an approximation, $C = 3.6 \times 10^{-10}$ for ferrite-pearlite steel. Fisher obtained very good correlation with test results by using a value of C equal to 2.05×10^{-10} (16). However, Rolfe uses the nominal stress rage, S_r, directly in

Eq. 5.3 for the $\Delta\sigma$ term (that is, $\Delta\sigma = S_r$) whereas Fisher includes a stress concentration factor, λ, in this term, such that $\Delta\sigma = \lambda S_r$ in Eq. 5.3. For the case of circular crack growth from a fillet weld crack, Fisher uses a value of λ equal to approximately 1.147.

Rolfe and Fisher both agree that a value of 3.0 for the constant n produces good correlation with test results. A range of values of n from 2.73 to 3.33 has been observed (2), resulting in a mean very close to 3.0.

If the values $f(g) = 2/\sqrt{\pi}$ and $n = 3$ are substituted into Eq. 5.3 the result is:

$$\frac{da}{dN} = C\left[\frac{2}{\sqrt{\pi}}\ \Delta\sigma\ \sqrt{a}\right]^3 \qquad (5.9)$$

Using Rolfe's value of C (3.6×10^{-10}) and $\Delta\sigma$ equal to S_r results in:

$$\frac{da}{dN} = 3.6 \times 10^{-10}\left[\frac{2}{\sqrt{\pi}}\ S_r\ \sqrt{a}\right]^3 \qquad (5.10)$$

Using Fisher's value of C (2.05×10^{-10}) and $\Delta\sigma$ equal to $\lambda \cdot S_r$, where $\lambda = 1.147$ gives:

$$\frac{da}{dN} = 2.05 \times 10^{-10}\left[\frac{2}{\sqrt{\pi}}\ (1.147\ S_r)\ \sqrt{a}\right]^3 \qquad (5.11)$$

If the term λ in Eq. 5.11 is taken outside of the parentheses and included in the C term, as in Eq. 5.10, then Eq. 5.11 becomes:

$$\frac{da}{dN} = 3.09 \times 10^{-10} \left[\frac{2}{\sqrt{\pi}} S_r \sqrt{a} \right]^3 \qquad (5.12)$$

Thus, it can be seen that Fisher's equivalent value of C is quite close to the general C value established by Rolfe for ferrite-pearlite steel.

Of the 18 beams tested in this phase of the program, nine failed due to cracks initiating in the flange-to-web fillet weld. The average initial flaw size, measured from these nine beams was approximately 0.053 in. This compares with Fisher's measured value of 0.040 in. (16). Using Eq. 5.12, the number of cycles to failure can be determined as:

$$\frac{da}{dN} = 3.09 \times 10^{-10} \left[\frac{2}{\sqrt{\pi}} S_r \sqrt{a} \right]^3$$

$$= 4.439 \times 10^{-10} S_r^{\,3} a^{1.5}$$

$$N = \int_{a_i}^{a_f} (0.225 \times 10^{10} S_r^{\,-3} a^{-1.5}) \, da$$

$$= 0.451 \times 10^{10} S_r^{\,-3} a_i^{\,-0.5}$$

$$= 1.959 \times 10^{10} S_r^{\,-3}$$

or $$\text{Log } N = 10.29 - 3 \text{ Log } S_r \qquad (5.13)$$

This equation is plotted on Fig. 5.1 together with the mean regression analysis line calculated for the same nine beams. It can be seen that the prediction line is in good agreement with that obtained from the test results, particularly at the lower stress range where a greater number of data points were available.

An average value of the constant C was calculated using the general equation, Eq. 5.9. For each beam which failed due to this type of crack, the measured initial crack size, a_i, was substituted into the equation, together with the stress range, S_r, and the number of cycles to failure, N, as observed for each test. The value of C was then calculated for each beam and an average value determined. This average C value was found to be 2.93×10^{-10}, which agrees very well with the value of 3.09×10^{-10} obtained using Eq. 5.12.

5.3.2 Cracks Initiating at Notch in Flange Tip

The stress intensity factor, K, for a single-edge-notched plate of finite width is given by Rolfe and Barsom as (14):

$$K = \sigma \sqrt{\pi a}\ f(a/b) \qquad (5.14)$$

where a/b is the ratio of the crack depth to one-half of the plate thickness. For a/b less than about 0.10, the value

of f(a/b) approaches 1.12. For beam GF-7, the depth of the notch at the flange tip was approximately 1/16 in., and the flange width was 6-3/4 in. Thus, the ratio a/b is 0.019 and f(a/b) will be approximately 1.12. The value of K will be:

$$K = 1.12\,\sigma\sqrt{\pi a}$$

or

$$K = \frac{3.52}{\sqrt{\pi}}\,\sigma\sqrt{a} \tag{5.15}$$

For a crack initiating in the fillet weld, the stress intensity factor as determined in Section 5.3.1 is:

$$K = \frac{2.0}{\sqrt{\pi}}\,\sigma\sqrt{a} \tag{5.16}$$

Since the cycle life, N, is proportional to $1/K^3$ for all types of fatigue cracks, then, for the same initial crack size, a beam with a crack initiating in the fillet weld will have a fatigue life considerably greater than an equivalent beam with a crack initiating at the flange tip. That is:

$$\frac{N_{fillet}}{N_{tip}} = \left(\frac{1}{2^3}\right) \Big/ \left(\frac{1}{3.52^3}\right) = 5.45$$

This assumes that the constant of proportionality of crack growth, C, is the same for both cases.

In specimen GF-7, the flaw size at the flange tip was larger than the average flaw size in the fillet welds. The notch depth was approximately 0.0625 in. as compared to 0.053 in. for the fillet weld flaws. Since N is proportional to $1/a_i^{0.5}$, then:

$$\frac{N_{fillet}}{N_{tip}} = \left(\frac{1}{0.053^{0.5}}\right) / \left(\frac{1}{0.0625^{0.5}}\right) = 1.09$$

Thus, if C is considered to be the same for the two cases, then it would be expected from the above analysis that:

$$\frac{N_{fillet}}{N_{tip}} = 5.45 \times 1.09 = 5.94$$

This says that the fatigue life of the edge-notched beam would be approximately one-sixth of an equivalent beam failing from a crack initiating in the fillet weld. This did not occur. Beam GF-7, which was tested at a stress range of 32 ksi, failed due to an edge crack at approximately 300,000 cycles. The mean fatigue life of the beams tested at 32 ksi, but failing from a fillet weld crack, was approximately 700,000 cycles.

There are several reasons which could account for the apparent increase in fatigue strength of an edge-notched beam over the strength predicted by fracture mechanics. The major reason is that the formula used to calculate K is intended for a sharp notch in the flange tip. In beam GF-7, the notch was

approximately 1/4 in. wide, which would result in a much lower stress concentration than that anticipated by the analysis. This is further confirmed by the fact that in several other beams which had similar size notches after fabrication, the flange tip was ground prior to testing over a width of several inches in order to reduce the stress concentration. The result was that the failure crack did not occur at this location.

Another reason for the discrepancy between the fracture mechanics predictions and test results may be that the value of C chosen is incorrect. In the above comparison it was assumed that C was the same for both cases. However, in the weld area and the adjacent heat-affected-zone, the constant of proportionality of crack growth (C) could be different from that at the flange tips, due to a possible phase change in the microstructure of the steel.

A third reason could be the fact that the stress intensity factor (K) changes as the crack gets quite large. For the edge-notched crack a value of 1.12 was used for f(a/b) at crack initiation. This value will change as a/b increases. However, this should not be a significant factor since the majority of the fatigue life of the beam is consumed when the crack size, a, is quite small.

Thus, this analysis tends to illustrate that fatigue crack growth will be much more rapid from a notch in the flange tip than from a crack initiating in a fillet weld flaw. The

ability to predict the fatigue life of the edge-notched beam using fracture mechanics is difficult, however, due mainly to the problem of evaluating the stress concentration factor.

5.3.3 Cracks Initiating at Toe of Groove Weld Reinforcement

The stress intensity factor, K, for a single-edge-notched plate of finite width can again be utilized for analysis of this type of crack. It was given previously (Eq. 5.14) as $K = \sigma \sqrt{\pi a}\ f(a/b)$.

The six beams which failed from this type of edge crack had no observable flaws or notches at the flange tip where the crack initiated. The initial crack size could thus be taken as the surface-roughness value due to the gas cutting process during fabrication. The usual range of surface-roughness values for this process is given as ASA 500 to ASA 1000 (17). Taking a value in the middle of this range would give a roughness height at the flange tip of 0.00075 in. If this is taken as the initial crack depth, then the ratio a/b will be very small and f(a/b) will be approximately 1.12. This will result in K having the same value as that obtained in the previous section (Eq. 5.15), that is $K = (3.52/\sqrt{\pi})\ \sigma \sqrt{a}$.

These six beams all failed from edge cracks which initiated at the toe of the groove-weld reinforcement. It has been shown that a concentration of stress occurs due to an abrupt change in the cross-sectional area of a plate or beam (18,19).

The magnitude of this local stress concentration depends on the height and length of the projection (measured parallel to the direction of stress), the curvature at the thickness transition, and the thickness of the plate. For a ratio of half the projection length to the radius of curvature, of 6.0, Neuber gives a stress concentration factor of approximately 1.5 (18). For ratios of radius of curvature to the plate thickness of 0.15, and height of projection to radius of curvature of 0.6, Popov gives a stress concentration factor of approximately 1.45 (19). These geometrical properties of the groove weld reinforcement are average values measured from beams which failed from a crack of this type.

If a stress concentration factor of 1.5 due to the thickness transition is included in the stress intensity factor for an edge-notched plate, then K becomes:

$$K = \frac{1.5 \times 3.52}{\sqrt{\pi}} \sigma\sqrt{a}$$

or

$$K = \frac{5.28}{\sqrt{\pi}} \sigma\sqrt{a} \qquad (5.17)$$

For comparison, the stress intensity factor for a crack initiating in the fillet weld, is (Eq. 5.16) $K = (2.0/\sqrt{\pi})\ \sigma\sqrt{a}$.

As described earlier, the notch depth for this type of crack will be taken as 0.00075 in. This is significantly less than the average flaw size in the fillet welds of 0.053 in. Since the cycle life, N, is proportional to $1/K^3$, then the

ratio of the fatigue life of beams with cracks initiating in fillet weld flaws to those with edge cracks initiating at the toe of the groove weld reinforcement will be:

$$\frac{N_{fillet}}{N_{as\text{-}welded}} = \frac{1}{(2.0^3)(0.53)^{0.5}} \Big/ \frac{1}{(5.28^3)(0.00075)^{0.5}}$$

$$= 2.18$$

This shows that the fatigue life of beams with as-welded groove welds should be approximately one-half of the life of a plain-welded beam. (This assumes that the value of C in Eq. 5.1 is the same for the two cases. The value could differ, however, for essentially the same reasons described in Section 5.3.2).

The ratio of fatigue lives is relatively insensitive to the value of initial crack depth (a_i) chosen for the as-welded groove weld case. If a_i were taken as 0.0005 in. or 0.001 in., corresponding to ASA 500 or ASA 1000 roughness values, then the ratio $N_{fillet}/N_{as\text{-}welded}$ would be 1.79 or 2.53, respectively.

The test results tend to confirm this strength reduction of approximately one-half, particularly for the two higher stress ranges. A fatigue strength reduction of one-half from the mean line of the plain-welded beam case would result in a line at approximately the 95% confidence limit for 95% survival. All the as-welded beams tested which failed from edge cracks had fatigue lives on, or slightly above, this 95% - 95% line.

It should be noted that stress category C, which most design specifications recommend for this type of detail, gives allowable fatigue strengths of approximately one-fifth of the plain-welded beam case (stress category B)(1,4,5,6). It would therefore appear to be a conservative classification of this detail.

This fracture mechanics analysis is useful for obtaining an approximate comparison between the fatigue strength of an as-welded groove-welded beam with that of a plain-welded beam. A quantitative prediction of the fatigue strength would be difficult to make however, due to the complicated task of accurately measuring the initial notch size, the weld reinforcement dimensions, and C, the constant of proportionality of crack growth.

5.3.4 Cracks Initiating at End of Bracing Attachment Detail

All of the beams in Phase 2 of the testing program failed from the same type of fatigue crack. All failures resulted from vertical cracks in the beam web at the end of the fillet-welded attachment. These cracks grew in a semi-elliptical shape from the toe of the fillet welds until they had progressed completely through the thickness of the web.

For a part-through thumbnail crack, Rolfe and Barsom give the equation for the stress-intensity factor as (14):

$$K = 1.12\,\sigma\sqrt{\pi\,\frac{a}{Q}} \qquad (5.18)$$

The value of 1.12 is a free-surface-correction factor. Q is an elliptic integral whose value depends on the ratio of crack depth to crack width. In one of the specimens, the fracture surface was cut open and examined prior to crack propagation through the web thickness. The ratio of crack depth to width was approximately 0.25 at that point. Rolfe evaluates Q for this ratio as approximately 1.4. Assuming that this ratio remains reasonably constant as the crack grows through the web, then the stress intensity factor will be:

$$K = \frac{2.97}{\sqrt{\pi}} \sigma \sqrt{a} \qquad (5.19)$$

There will also be a stress concentration factor due to the stress flow from the beam web to the attachment. Fisher et al.(3) have shown by means of a finite element analysis that when the attachment plate length exceeds 8 in., then the force in the attachment will reach essentially its full capacity, that is, the stress in the plate would be as calculated from flexural theory. Popov gives a stress-concentration factor of approximately 2.4 for a flat plate in tension with a fillet having an r/d value of zero, where r/d is the ratio of fillet curvature to plate thickness (19). As the attachment in this test series is rectangular in shape, the fillet radius will approach a value of zero. This stress concentration factor can be applied to the nominal stress, σ, to give a revised K value to include both the crack geometry effect plus the attachment stress flow effect.

The revised stress intensity factor will now be:

$$K = 2.4 \frac{2.97}{\sqrt{\pi}} \sigma\sqrt{a}$$

or

$$K = \frac{7.13}{\sqrt{\pi}} \sigma\sqrt{a} \qquad (5.20)$$

Signes et al. (20) showed that fatigue cracks initiate at the toes of fillet welds due to a slight undercut or due to slag inclusions along the fusion boundary. These defects may be regarded as sharp notches from which cracks initiate. They found the defects to be approximately 0.003 in. deep. In the tests by Fisher et al. (3) it was determined that the average initial crack size was about 0.004 in. for fillet-welded stiffeners. Using a value of a_i equal to 0.004 in. and the previously obtained value of $C = 3.09 \times 10^{-10}$, then Eq. 5.1 can be integrated to obtain an expression for the fatigue life of this type of detail:

$$\frac{da}{DN} = C(\Delta K)^n$$

$$= 3.09 \times 10^{-10} \left(\frac{7.13}{\sqrt{\pi}} S_r \sqrt{a}\right)^3$$

$$= 201.1 \times 10^{-10} S_r^{\,3} a^{1.5}$$

$$N = \int_{a_i}^{a_f} (4.97 \times 10^7 \, S_r^{-3} \, a^{-1.5}) \, da$$

$$= 9.94 \times 10^7 \, S_r^{-3} \, a_i^{-0.5}$$

$$= 0.157 \times 10^{10} \, S_r^{-3}$$

or

$$\text{Log } N = 9.196 - 3 \text{ Log } S_r \qquad (5.21)$$

This equation is plotted on Fig. 5.2 together with the mean regression analysis line calculated from the experimental results for Phase 2 of the program. It can be seen that there is good correlation between the experimental results and the estimate obtained using fracture mechanics, particularly at the higher stress ranges where there were a larger number of data points.

5.4 Effect of Weld Reinforcement Angle on Fatigue Strength

Gurney found that there was a quantitative correlation between weld reinforcement angle and fatigue strength of plate specimens with transverse groove welds (7). He measured the obtuse angle between the plate surface and the tangent to the reinforcement at its point of contact with the plate surface. It was observed that failure usually originated at the point of minimum angle, that is, where the thickness transition was most abrupt. When the reinforcement angle was plotted against stress

range for specimens failing at two million cycles, it was found that the results fell within a narrow scatter band. The upper end of this band (that is, with a reinforcement angle of 180°), was the fatigue strength of a plain plate without a transverse splice.

Figure 5.3 shows a plot of reinforcement angle, θ, versus the cube root of number of cycles to failure ($N^{1/3}$) for the six beams in Phase 1 of this test program which failed at the groove weld. The cube root of N was used in this plot since N is proportional to S_r^{-3}, and stress range was maintained as the independent variable for these tests, whereas in the tests conducted by Gurney N was the independent variable. Thus, the plot is essentially a comparison of θ and S_r as was done by Gurney. (The "w" designation following some specimen numbers indicates that the crack initiated at the inside face of the tension flange. These values were then adjusted to an equivalent value at the extreme fibre of the beam so that S_r was maintained at a constant value.) The values shown in Fig. 5.3 for $\theta = 180°$ are the cube root of the fatigue lives for plain-welded beams as taken from Fisher's work (2). Two lines are plotted corresponding to the results from the two stress ranges of 25 and 32 ksi, with the plain-welded beam values giving an upper limit to the fatigue strength.

As can be seen in Fig. 5.3, the lines corresponding to the two stress ranges are almost parallel, with all of the data points falling very close to the lines. This relationship

illustrates the importance of the weld reinforcement shape. Although all of these groove welds would be considered as acceptable in welding practice, different reinforcement angles can result in significantly different fatigue strengths. The present Canadian Standard Specifications for Welding of Steel Structures (CSA W59.1) only specifies that the maximum height of the groove weld reinforcement be less than 1/8 in. (29). (In this test program the maximum height measured on a specimen was 1/16 in.) No reference is made in the specification to the reinforcement angle nor to the length of the weld reinforcement profile.

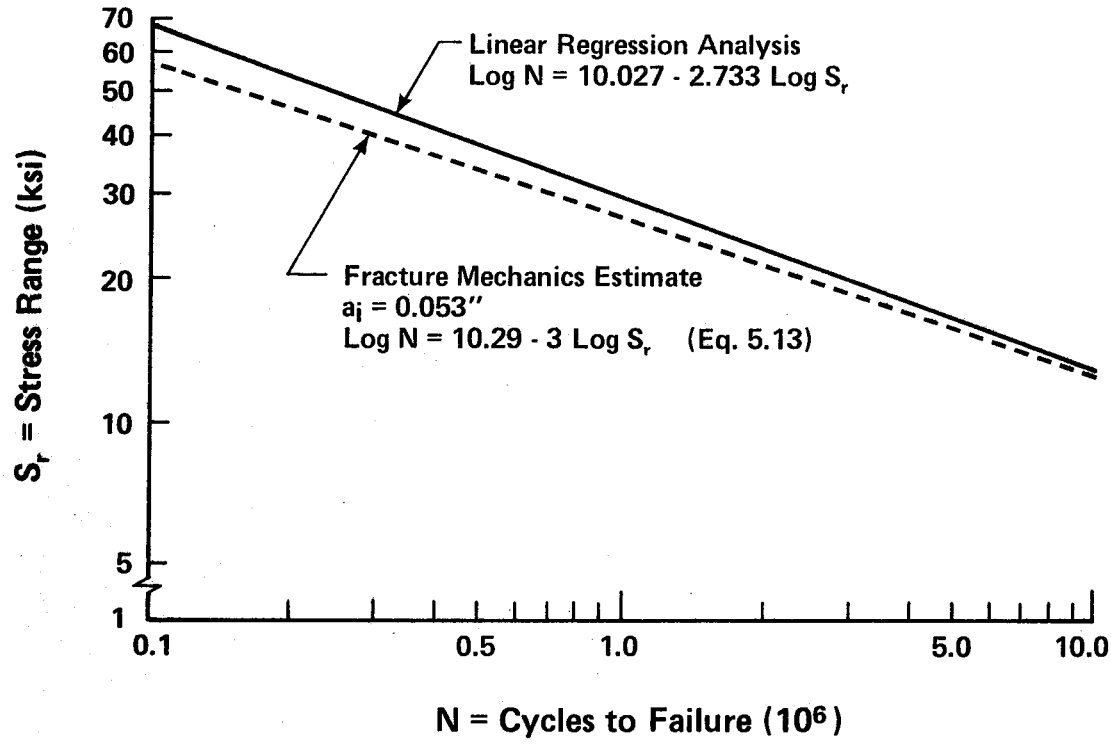

FIGURE 5.1 BEAMS FAILING FROM CRACK IN FLANGE-TO-WEB FILLET WELD

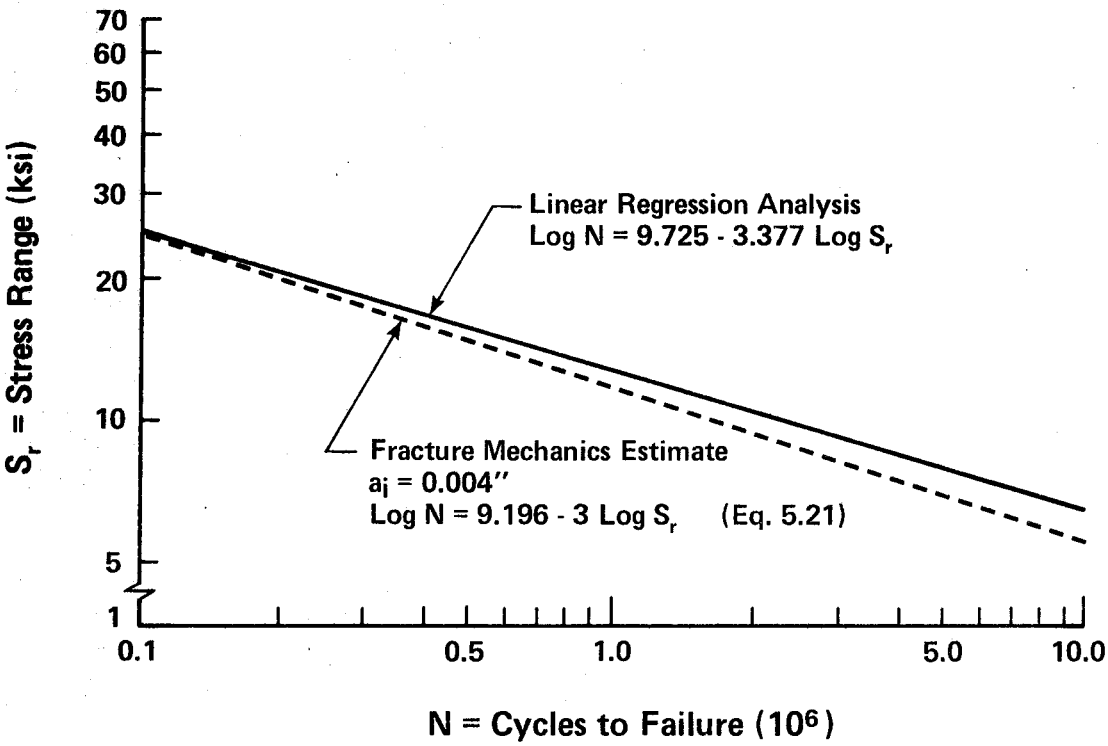

FIGURE 5.2 BEAMS WITH LATERAL BRACING ATTACHMENTS

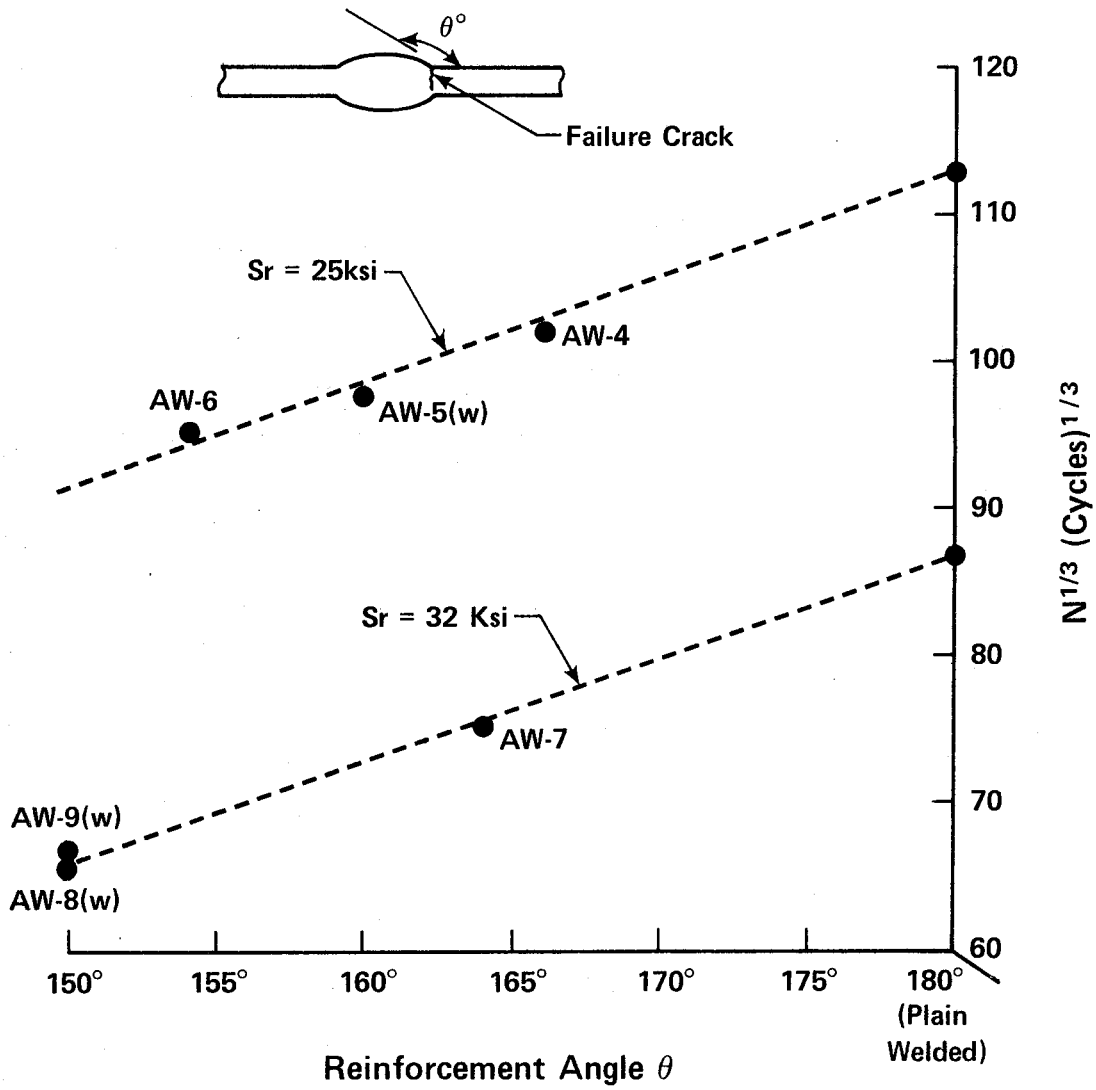

FIGURE 5.3 RELATIONSHIP BETWEEN REINFORCEMENT ANGLE AND FATIGUE STRENGTH

CHAPTER VI

SUMMARY AND CONCLUSIONS

6.1 Summary

This investigation has examined the influence of two different types of welded details upon the fatigue strength of steel beams. Phase 1 was the examination of beams with groove-welded flange splices while Phase 2 was the examination of beams with horizontal bracing attachments fillet-welded to the web. The experimental aspect of this program consisted of tests on 18 welded wide-flange beams in Phase 1, and seven hot-rolled wide-flange beams in Phase 2. Details examined in the first phase included the effects of grinding the groove weld reinforcement flush versus leaving the splice as-welded. In the second phase, both the effect of the horizontal attachment detail itself and the influence of lateral bracing attached to the detail was examined. The experimental results were analysed statistically and compared with fracture mechanics predictions of the fatigue lives. A comparison was made with the results of previous investigations of welded details and also with the recommendations in current design specifications.

6.2 Conclusions

The following conclusions are drawn, based on the findings of the investigation.

6.2.1 General

1. For the details tested in this program, it was found that the number of cycles to failure is approximately proportional to the inverse of the stress range taken to the third power, that is,

$$N \alpha \frac{1}{S_r^3}$$

This was substantiated by means of a statistical analysis of the test results and also by means of fracture mechanics predictions.

2. The linear model, $\text{Log } N = B_1 + B_2 \text{ Log } S_r$, provided good correlation with the test results.

3. The linear regression analysis for the details tested resulted in a family of nearly parallel lines when plotted on a log-log scale of stress range versus number of cycles. These lines were also found to be parallel to those obtained in earlier studies on other details (2,3), and had a negative slope of about 3.0.

4. The fracture mechanics analysis, based on crack propagation from existing flaws, substantiated the linear model and provided a reasonable explanation of the test results.

5. There were no observable differences in the fatigue life of a detail due to interruptions of the test for periods of time of up to one week in duration. Other

variables, such as laboratory temperature and humidity, did not appear to have any influence on the fatigue life.

6.2.2 Phase 1 (Beams with Groove-Welded Splices)

1. Beams with the groove weld reinforcement ground flush with the profile of the flange had the same fatigue strength and type of failure crack as a plain-welded beam with no splice.
2. Beams with the groove weld reinforcement left as-welded had a slightly lower mean fatigue strength and a different type of failure crack than a plain-welded beam. The majority of these beams did, however, have strengths substantially above those predicted by current North American specifications.
3. The standard deviation and limits of dispersion were less for the as-welded beams than for the ground flush beams. This resulted in the 95% confidence limits for 95% survival being almost the same for the two details.
4. The abruptness of the groove weld reinforcement, as measured by the obtuse angle between the tangent to the toe of the weld and the plate surface, was shown to have a considerable influence on the fatigue strength. The more abrupt the thickness transition, the lower was the fatigue life.

5. Fatigue cracks in beams with the groove weld reinforcement ground flush generally initiated at flaws in the flange-to-web fillet weld. These flaws were relatively small and could not be detected by visual inspection. A major flaw in one beam resulted in a fatigue strength slightly below that expected for this category of detail.
6. Edge notches at the flange tips resulted in considerably lower fatigue strengths and a different type of failure crack than the equivalent beams without notches. Grinding out these notches with a gradual transition eliminated this effect.
7. A groove weld undercut in an as-welded beam resulted in a considerable strength reduction from that of an equivalent beam without a groove weld flaw. This flaw was detected by means of an X-ray inspection but the subsequent repair was not satisfactory.

6.2.3 Phase 2 (Beams with Lateral Bracing Attachments)

1. All beams in this phase of the program failed due to a vertical fatigue crack which initiated at the toe of the attachment fillet weld and grew through the beam web.
2. The fatigue strength of these beams was essentially the same as that of a cover-plated beam.

3. All beams had fatigue strengths greater than those which would be predicted by current North American specifications.
4. The attachment of bracing to the lateral gusset detail had no observable influence on the fatigue strength of the beams.

6.3 Recommendations

The following recommendations are made relative to CSA Standard S6-1974, Supplement No. 1 - 1976, CSA Standard S16.1 - 1977, and AASHTO Standard Specification for Highway Bridges 1977.

1. Beams with groove-welded splices in which the weld reinforcement is ground flush with the profile of the flange should continue to be designed as fatigue category B.
2. Beams with groove-welded splices in which the weld reinforcement is left as-welded could also be designed as category B since the 95% confidence limit for 95% survival is approximately the same for this class as for flush-ground groove welds. Alternatively, another category between B and C could be established for as-welded groove welds.
3. Design specifications for fatigue should include inspection provisions to detect and repair any sharp notches in beam flanges and other tensile load carrying members.

4. Further studies should be made on beams with groove-welded splices with the weld reinforcement left as-welded. These should include tests on splices with thickness and/or width transitions.
5. Fatigue category E should continue to be used in design specifications for fillet-welded attachment details wherein the detail length in the direction of stress is greater than 12 times the plate thickness or greater than 4 in.
6. Further studies should be made on beams with other types of lateral bracing attachments. These should include tests on beams with groove-welded attachments.
7. Further studies should be made on beams with bracing members attached to the lateral gusset details. These studies should include a more extensive investigation of bracing stiffnesses and differential deflections between beams of actual steel bridges.

REFERENCES

1. *Interim Standard Specification for Highway Bridges,* American Association of State Highway and Transportation Officials, Washington, 1974.

2. Fisher, J.W., Frank, K.H., Hirt, M.A., and McNamee, B.M., *Effect of Weldments on the Fatigue Strength of Steel Beams",* NCHRP Report 102, 1970, Transportation Research Board, Washington.

3. Fisher, J.W., Albrecht, P.A., Yen, B.T., Klingerman, D.J., and McNamee, B.M., *Fatigue Strength of Steel Beams with Welded Stiffeners and Attachments,* NCHRP Report 147, 1974, Transportation Research Board, Washington.

4. *Standard Specification for Highway Bridges,* American Association of State Highway and Transportation Officials, Washington, 1977.

5. *Design of Highway Bridges,* CSA Standard S6-1974, Supplement No. 1 - 1976, Canadian Standards Association, Rexdale, Ontario, Canada.

6. *Steel Structures for Buildings - Limit States Design,* CSA Standard S16.1-1974, Canadian Standards Association, Rexdale, Ontario, Canada.

7. Gurney, T.R., *Fatigue of Welded Structures,* British Welding Research Association, London, 1968.

8. Munse, W.H., *Fatigue of Welded Steel Structures,* Welding Research Council, New York, N.Y., 1964.

9. Munse, W.H., and Stallmeyer, J.E., *Fatigue in Welded Beams and Girders,* Bulletin 315, Highway Research Board, Washington, 1962.

10. Yamada, K., and Albrecht, P., *Fatigue Behavior of Two Flange Details,* Journal of the Structural Division, American Society of Civil Engineers, Vol. 103, No. ST4, April 1977.

11. Fisher, J.W., Pense, A.W., and Roberts, R., *Evaluation of Fracture of Lafayette Street Bridge,* Journal of the Structural Division, American Society of Civil Engineers, Volume 103, No. ST7, July 1977.

12. Fisher, J.W., *Bridge Fatigue Guide - Design and Details,* American Institute of Steel Construction, New York, N.Y., 1977.

13. McGuire, W., *Steel Structures,* Prentice-Hall, Inc., New Jersey, 1968.

14. Rolfe, S.T., and Barsom, J.M., *Fracture and Fatigue Control in Structures - Applications of Fracture Mechanics,* Prentice-Hall, Inc., New Jersey, 1977.

15. Shanley, F.R., *A Proposed Mechanism of Fatigue Failure,* Colloquium on Fatigue - International Union of Theoretical and Applied Mechanics, Stockholm, 1955.

16. Fisher, J.W., *Fatigue Strength of Welded Steel Beam Details and Design Considerations,* Proceedings of the Canadian Structural Engineering Conference, Montreal, Canada, 1972.

17. Baumeister, T., Editor, *Standard Handbook for Mechanical Engineers,* McGraw-Hill, New York, N.Y., 1967.

18. Neuber, H., *Theory of Notch Stresses; Principles for Exact Stress Calculation,* Translated from the German for the David Taylor Model Basin, U.S. Navy, by F.A. Raven, Ann Arbor, 1946.

19. Popov, E.P., *Introduction to Mechanics of Solids,* Prentice-Hall Inc., New Jersey, 1968.

20. Signes, E.G., Baker, R.G., Harrison, J.D., and Burdekin, F.M., *Factors Affecting the Fatigue Strength of Welded High Strength Steels,* British Welding Journal, Vol. 14, March 1967.

21. Paris, P.C., and Erdogan, *A Critical Analysis of Crack Propagation Laws,* Transactions of the ASME, Journal of Basic Engineering, Series D, 85, No. 3, 1963.

22. Irwin, G.R., *Analysis of Stresses and Strains Near the End of a Crack Transversing a Plate,* Transactions, ASME, Journal of Applied Mechanics, Vol. 24, 1957.

23. Dorton, R.A., Holowka, M. and King, J.P.C., *The Conestogo River Bridge - Design and Testing,* Canadian Journal of Civil Engineering, National Research Council Canada, Volume 4, Number 1, March 1977.

24. Dorton, R.A., Csagoly, P.F., *The Development of the Ontario Bridge Code,* Ontario Ministry of Transportation and Communications, October 1977.

25. Gurney, T.R., *Fatigue Tests on Butt and Fillet Welded Joints in Mild and High Tensile Structural Steels,* British Welding Journal, Vol. 9, No. 11, November, 1962.

26. Gurney, T.R., *Further Fatigue Tests on Mild Steel Specimens with Artificially Induced Residual Stresses,* British Welding Journal, Vol. 9, No. 11, November 1962.

27. Gurney, T.R., *Fatigue Strength of Beams with Stiffeners Welded to the Tension Flange,* British Welding Journal, Vol. 7, No. 9, September 1960.

28. Fisher, J.W., Yen, B.T., *Design, Structural Details and Discontinuities in Steel,* ASCE Specialty Conference on Safety and Reliability of Metal Structures, Pittsburgh, Pa., November 1972.

29. *General Specification for Welding of Steel Structures (Metal-Arc Welding),* CSA Standard W59.1-1970, Canadian Standards Association, Rexdale, Ontario, Canada.

APPENDIX A

DEFLECTION MEASUREMENTS OF TWO HIGHWAY BRIDGES

A.1 Purpose and Scope

Prior to the testing in Phase 2 of the program it was decided to obtain an estimate of deflections and stiffnesses of actual bridges in order to simulate these conditions in the laboratory testing. Secondary stresses are induced in the bracing attachment details due to forces in the bracing members caused by differential girder deflections. The magnitude of these stresses depends on the gusset plate thickness, the sizes and lengths of the bracing members, and the magnitude of the differential vertical girder deflections. If the bracing members are long and slender, then the majority of the bracing member force will be absorbed by the bending of the member and little will be transferred to the gusset plate. Conversely, a short and/or heavy bracing member will transfer a considerable force to the gusset plate. These considerations prompted the field investigation.

A literature survey failed to uncover any valid study of maximum differential girder deflections of steel beam highway bridges under heavy truck loading. Such problems as lateral load distribution and lane position made accurate analysis of the deflections difficult. It was decided, therefore, to conduct a field survey of two highway bridges in the Edmonton area

which were known to be subjected to high frequency of heavy truck loading in order to determine differential girder deflections and also to measure bracing member stiffnesses.

A.2 Experimental Program

Deflection measurements were taken on two bridges in the Edmonton area, the Entwistle Bridge and the Red Deer River Bridge. These bridges were selected on the basis of access to the underside of the deck, volume of heavy traffic and type of bridge. Measurements were made over a two-day period at each bridge.

Deflection readings were taken only in the end spans of each bridge. The Entwistle Bridge has an 80 ft simply-supported end span which uses steel plate girders approximately six ft deep spaced at 12 ft centres. The deck is a seven in. non-composite reinforced concrete slab. Lateral bracing consists of two 4 x 4 x 5/16 in. angles which are attached to the vertical stiffeners approximately six in. above the bottom flange.

The Red Deer River Bridge has a 120 ft end span, simply-supported at one end and continuous at the other. The steel plate girders are approximately eight ft deep and are spaced at 20 ft centres. An eight in. thick reinforced concrete slab acts compositely with the girders. The lateral bracing consists of two WT4 x 8.5 sections framing perpendicular to the girders and attached to the vertical stiffeners and two WT7 x 17 sections framing diagonally into a horizontal gusset plate located immediately above the bottom flange.

Deflection readings were taken under each girder at the point where deflection would be a maximum. Figures A.1 and A.2 show the field set-up for obtaining deflection readings. A small diameter steel cable strand was attached by means of a magnetic base to the bottom flange of each girder. The cable extended through a guide bar and a lead weight was attached below the bar on the opposite end of the cable. The guide bar was fixed by means of a magnetic base to a level steel platform on the ground. As the girder deflected under load, the cable moved through the guide bar. A rubber slip ring marked the amount of this movement.

The licensed gross weight of the vehicles and their lane position on the bridge was recorded. Deflection measurements were taken under each girder only for the heavier vehicles. This included trucks with registered gross weights of from 80,000 to 110,000 pounds. Approximately 40 deflection readings were taken on the Entwistle Bridge and 25 on the Red Deer River Bridge.

A.3 Test Results

The maximum differential deflection between girders at the Entwistle Bridge was about 0.100 in., while that obtained at the Red Deer River Bridge was about 0.165 in.

The girders on the Entwistle Bridge were spaced at 12 ft centres. Thus, a rotation of about 0.04 degrees was

induced in the lateral bracing under the 0.100 in. differential vertical deflection. If the bracing is assumed to deflect as a cantilever between girders, then the end deflection would be $(PL^3)/(3EI)$. The stiffness of the bracing could therefore be taken as approximately equal to $(3EI)/L^3$. Using the measured sizes of lateral bracing on the Entwistle Bridge, this stiffness value would be about 0.14 k/in.

The girders on the Red Deer River Bridge were at 20 ft centres. A rotation of about 0.04 degrees was again induced in the bracing at the attachment detail under 0.165 in. deflection. The stiffness value of the lateral bracing would thus be about 0.19 k/in.

In the testing program reported herein, the maximum beam deflections ranged from 0.160 in. for the 9 ksi stress range at the gusset level to 0.260 in. for the 19 ksi stress range. These deflections would result in rotation angles of 0.12 and 0.21 degrees respectively. The use of the two 2-1/2 x 2-1/2 x 3/8 in. angles at a 70 in. bracing length gives a stiffness value of about 0.29 k/in. When the two 2-1/2 x 2-1/2 x 1/4 in. bracing angles at a 25 in. length were used the value was 7.61 k/in.

Comparing the values measured in the field with those used in the test program, it can be seen that the majority of the tests (those with 3/8 in. bracing angles at a 70 in. bracing length) were conducted with differential deflections and bracing stiffnesses equal to, or greater than, the values of the two

actual bridges investigated. The deflections were of the same magnitude but the rotation angles and bracing member stiffnesses were slightly greater. These greater stiffnesses should result in a more critical fatigue situation as more force will be transferred to the attachment detail on the test beam, consequently producing higher secondary stresses. The one beam which was tested with 1/4 in. angles and a 25 in. bracing length would be a considerably more critical situation for fatigue than would normally be encountered.

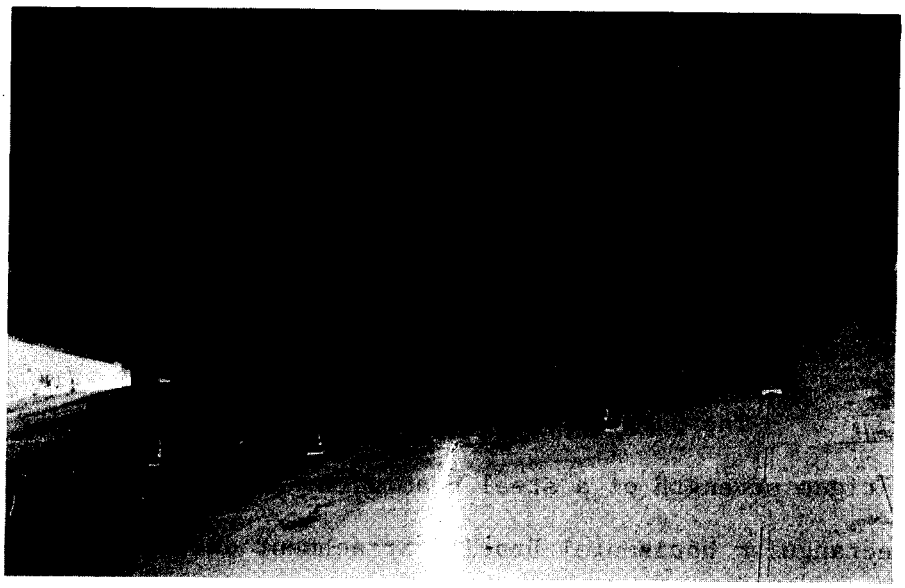

FIGURE A.1 DEFLECTION GAUGE SET-UP UNDER BRIDGE DECK

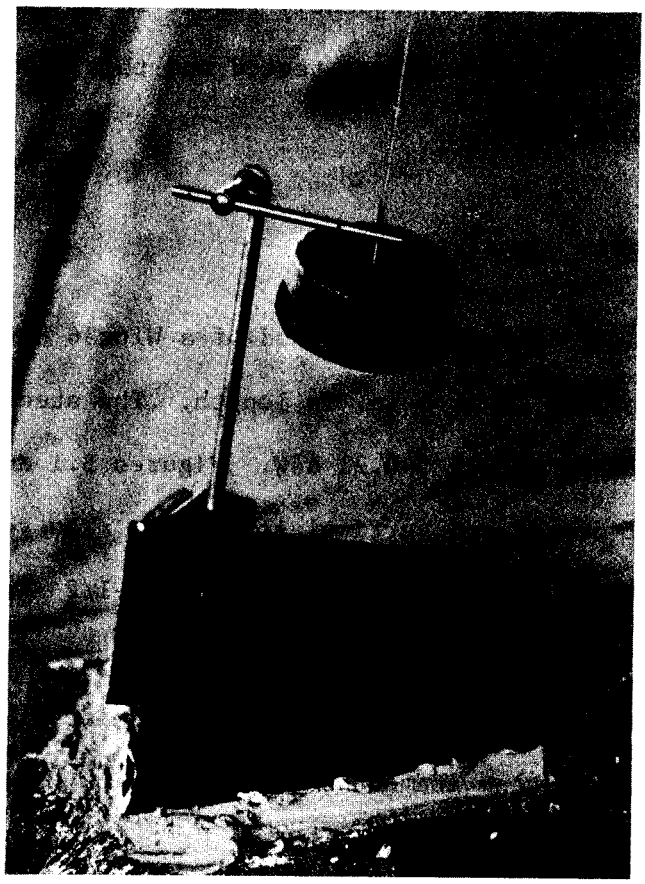

FIGURE A.2 DEFLECTION GAUGE

APPENDIX B

A PILOT STUDY ON BEAMS WITH TAPERED LATERAL BRACING ATTACHMENTS

B.1 Scope

The purpose of this pilot study was to examine the fatigue strength of a steel beam with a tapered, rather than rectangular horizontal bracing attachment detail. It was considered that a tapered transition in the gusset plate might reduce the stress concentration effect at the termination of the fillet weld toe and consequently result in an increased fatigue strength. Only one beam was tested and this beam contained only one such detail.

B.2 Specimen Description

The test beam consisted of a W16x36 hot-rolled wide flange section, 10 ft 6 in. in length. The steel met the specifications of CSA G40.21 44W. Figures B.1 and B.2 show the attachment detail and vertical stiffener. The vertical stiffener was a 3/8 in. plate, 3-1/4 in. wide by 13-1/2 in. long and it was located at the centreline of the beam span on one side of the web only. The stiffener was fillet welded to the top flange and web of the beam and had a 1 in. by 1 in. cope cut out at the flange-to-web junction.

As shown in Fig. B-1, the horizontal gusset plate was a 5/16 in. thick plate with 2:1 tapers on either side of a 10 in. long central section. (The central section had the same dimensions as the gusset plate attachment used in Phase 2 of the test program.) The gusset was slotted to fit around the vertical stiffener and was then fillet welded to the beam web and to the stiffener. A 1 in. by 1 in. cope was cut out of the centre portion of the gusset to prevent contact between the web and stiffener welds. The gusset plate was attached at a distance of 2-7/16 in. from the extreme fibre of the beam to the underside of the gusset.

All welds were done manually by the shielded-metal-arc process using AWS E70XX electrodes. They were done at the University of Alberta Structural Engineering Laboratory by a welder certified by the Canadian Welding Bureau. All fillet welds were 1/4 in. in size and were inspected visually prior to testing.

B.3 Test Set-Up

The test set-up for the beam containing this detail was the same as that described in Section 3.3.2 for the rectangular gussets except that the distance between load points was 3 ft 6 in.

No bracing was attached to the gusset plate since the work done under Phase 2 had shown that attachment of lateral bracing produced no discernible effect on fatigue life. The application and measurement of load was similar to that described for the Phase 1 tests.

B.4 Testing Procedure

A stress range of 13 ksi at the level of the gusset plate with a minimum stress of 2.8 ksi was maintained for this test. Static tests were carried out prior to the fatigue testing. These were conducted in the same manner as described for Phase 2 of the main test program. The failure criterion was the same as that used in Phase 2.

B.5 Test Results

Fatigue cracks occurred at the fillet weld toes at both ends of the gusset plate attachment. As in Phase 2 of the test program, the cracks grew vertically, both upward and downward in the beam web, and eventually through to the opposite side of the web. Figure B.3 shows one of the fatigue cracks.

Both of the fatigue cracks occurred at approximately the same number of cycles. The fatigue lives were 714,000 and 744,000 cycles for the two failure cracks. When plotted on a log-log graph of stress range versus number of cycles, these two points fell very close to the mean regression line for cover-plated beams shown in Fig. 4.20. This was also very close to the mean regression line for the test results of Phase 2.

The results of the static load tests are shown in Fig. B.4. Comparing this with Fig. 4.19 it can be seen that considerably more force is being transferred through the gusset plate than was the case with the rectangular attachments of

Phase 2. It should be noted that the stresses at the beam web are essentially the same.

B.6 Discussion

The results of this pilot test indicate that no additional fatigue strength is gained by using a tapered gusset plate as compared to a rectangular one. Although the stress flow through this tapered attachment was significantly different, the fatigue lives were essentially the same as the beams tested in Phase 2.

It appears that the notch-producing detail at the toe of the fillet weld together with the stress in the beam web at this point govern the fatigue life. The defects at the weld toe, such as an undercut or a slag inclusion, will be essentially the same with both types of details. Thus, in order to improve the fatigue strength with this tapered attachment, it would probably be necessary to grind the fillet weld in order to conform with the tapered slope and also to remove any notch-producing defects in this region.

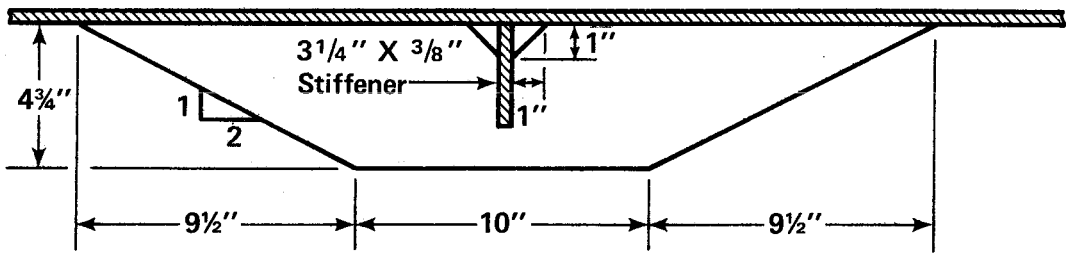

Section A-A

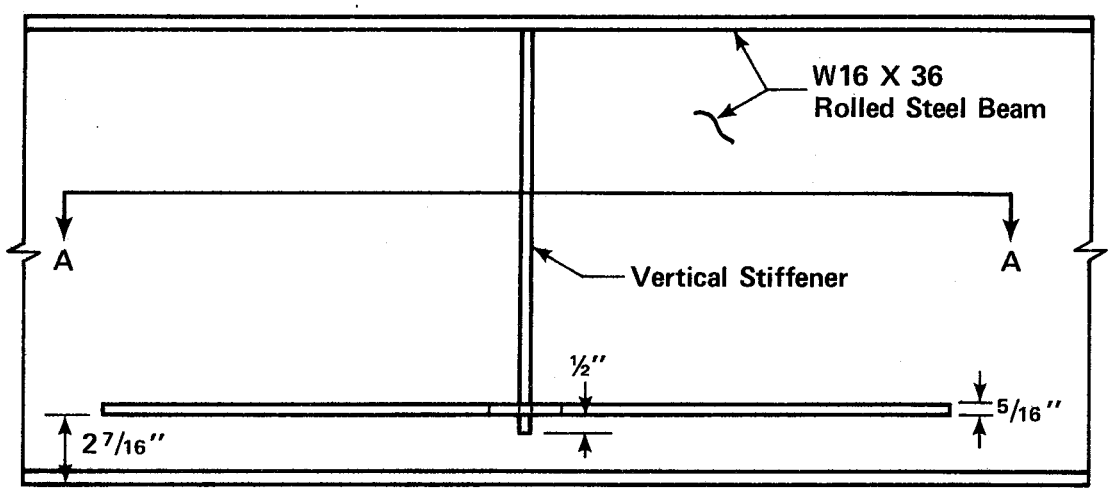

Elevation

FIGURE B.1 PILOT STUDY: TAPERED ATTACHMENT DETAIL

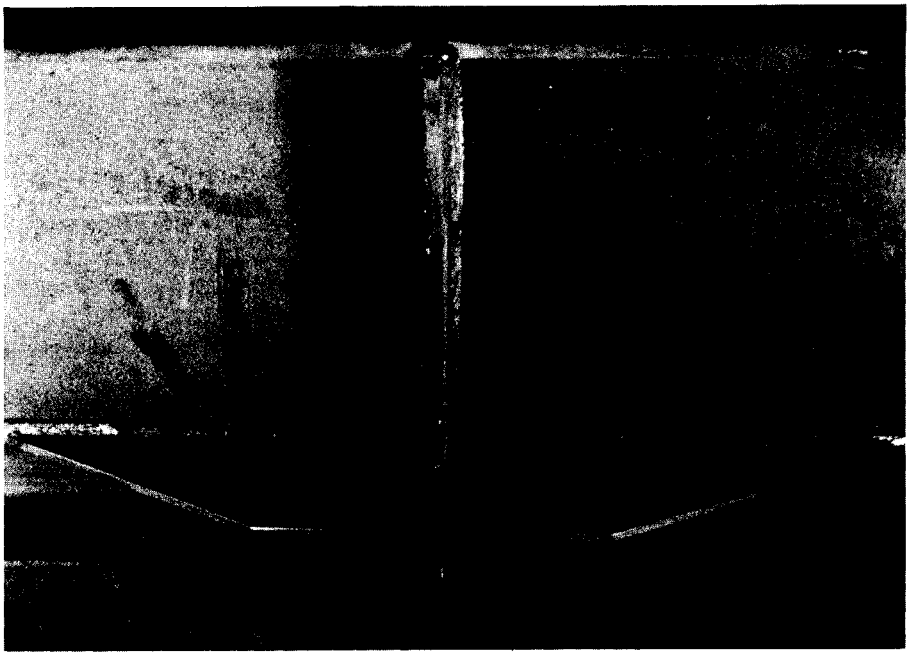

FIGURE B.2 TAPERED ATTACHMENT DETAIL

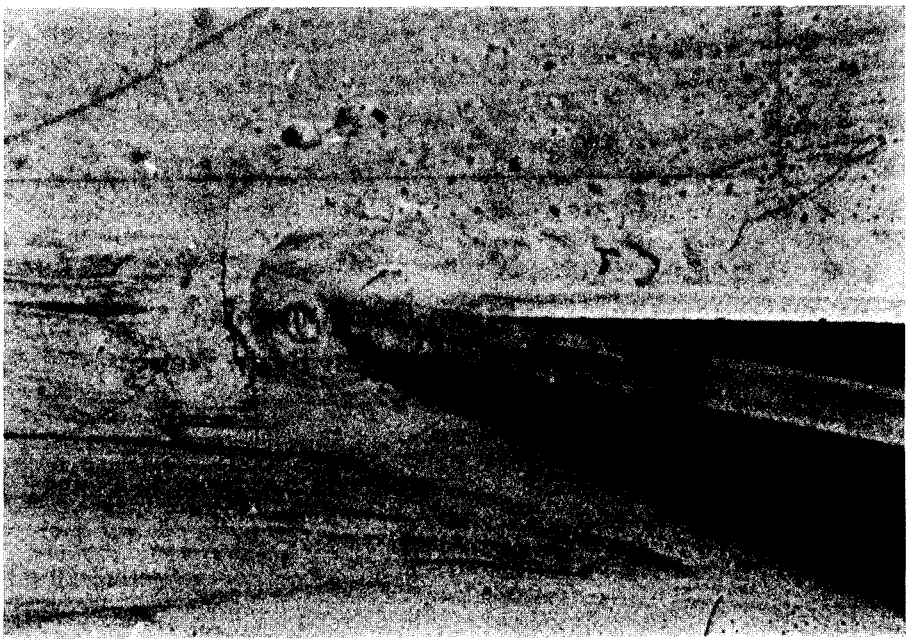

FIGURE B.3 FATIGUE CRACK AT TOE OF ATTACHMENT FILLET WELD

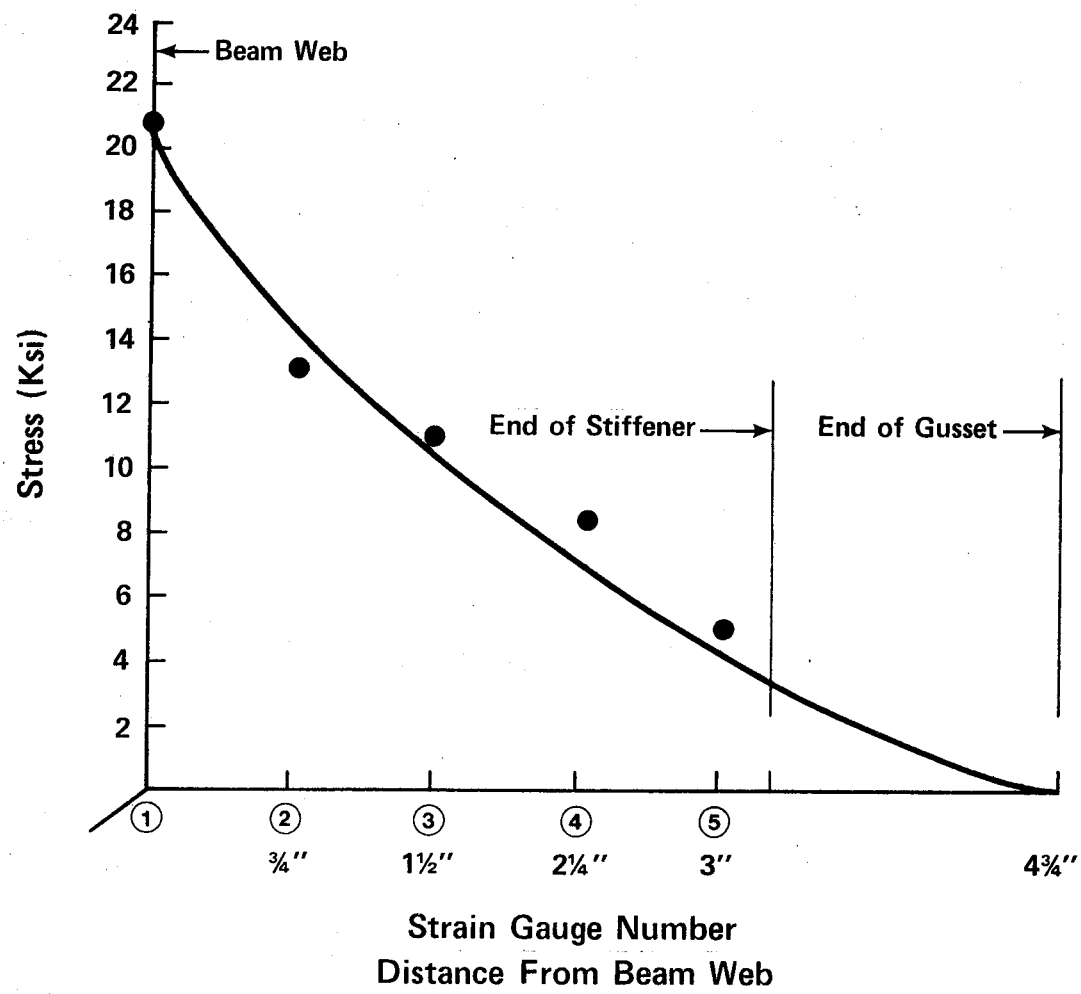

FIGURE B.4 STRESS DISTRIBUTION IN TAPERED GUSSET PLATE